공학박사학위논문

A Study on the Design Procedure for Efficient Flare System through Dynamic Analysis of Abnormal Condition

비정상 상태의 동적 분석을 통한 효율적인 플레어 시스템 설계 방법론 연구

2012년 8월

서울대학교 대학원

화학생물공학부

박경태

Abstract

A Study on the Design Procedure for Efficient Flare System through Dynamic Analysis of Abnormal Condition

Kyungtae Park
School of Chemical and Biological Engineering
The Graduate School
Seoul National University

Reasonable relief load estimation is a crucial task in industry since it will affect a flare system design. If a relief load is overestimated, resources will be wasted since a flare system is very huge, costly system and it operates at an emergency situation. However, if a relief load is underestimated, it will cause a catastrophic accident since a flare system protects whole plant from various overpressure events.

American Petroleum Institute (API) have tried to set up the guideline for a relief load estimation method through API standard 520 and 521, there is still much room for interpretation. In industry, the heat and material balance method is widely used in order to estimate a relief

load since it gives logical estimation results. However, this method tends to overestimate the relief load since it is very conservative method.

Nowadays, there are several attempts to apply a dynamic analysis by using a dynamic simulator in order to estimate relief loads since a dynamic simulation can give information of an unsteady situation. Therefore, an implementation of a dynamic simulation in order to estimate relief loads is expected to give rigorous and precise results since the relief occurs under unsteady situations.

In this research, the relief load estimations were performed by using the heat and material balance method and the dynamic simulator (HYSYS). In addition, the combination effect of High Integrity Protection Systems (HIPS) and the dynamic simulation was investigated in order to reduce the relief load. And the liquid fractionation unit and the xylene fractionation and the PAREX unit were selected for case studies. Finally, the new design procedure for the efficient flare system design was proposed.

Keywords: Flare Design, Relief Load Estimation, Dynamic Simulation and High Integrity Protection Systems (HIPS)

Student Number: 2008-21074 **Name: Kyungtae Park**

TABLE OF CONTENTS

1. Introduction 1

2. Background Theories

2.1. Relief Load Estimation by Using the Heat and Material Balance Method 9

2.2. Dynamic Simulator.....13

2.2.1. General Descriptions 13

2.2.2. Mathematical Model in a Dynamic Simulator.....16

2.3. High Integrity Protection Systems (HIPS) 19

2.3.1. General Descriptions 19

2.3.2. Calculation Method of Probability of Failure on Demand (PFD) of HIPS.....23

2.3.2.1. 1 Out of 1 System 24

2.3.2.2. 1 Out of 2 System 25

2.3.2.3. 2 Out of 2 System 26

2.3.2.4. 2 Out of 3 System 26

2.4. Fault Tree Analysis (FTA).....27

2.4.1. General Descriptions 27

2.4.2. Minimal Cut Set Approach 30

3. Relief Load Estimation by Using the Heat and Material Balance Method

3.1. Relief Load Estimation for the Liquid Fractionation Unit.....32

3.1.1. Relief Load Estimation from a Single Source 35

3.1.2. Relief Load Estimation from Multiple Sources 48

3.1.3. Relief Load Estimation Results Summary for a Liquid Fractionation Unit.....53

3.2. Relief Load Estimation for the Xylene Fractionation Unit and the PAREX Unit 54

3.2.1. Relief Load Estimation from a Single Source 57

3.2.2. Relief Load Estimation from Multiple Sources 63

3.2.3. Relief Load Estimation Results Summary for the Xylene Fractionation and the PAREX Unit 65

4. Relief Load Estimation by Using the Dynamic Simulator

4.1. Relief Load Estimation for a Liquid Fractionation Unit ...67

4.1.1. Relief Load Estimation from a Single Source 72

4.1.2. Relief Load Estimation from Multiple Sources 77

4.1.3 Results Summary.....80

4.2. Relief Load Estimation for a Xylene Fractionation Unit and the PAREX unit.....82

4.2.1. Relief Load Estimation from a Single Source 82

4.2.2. Relief Load Estimation from Multiple Sources 87

4.2.3 Results Summary 91

5. Discussion Regarding Results of the Relief Load Estimation.....93

5.1. The Liquid Fractionation Unit 93

5.2. The Xylene Fractionation Unit and the PAREX Unit 95

5.3. Discussion 97

6. Relief Load Mitigation Using HIPS 99

6.1. General Description.....99

6.2. HIPS Application to the Liquid Fractionation Unit 100

7. The Effect of the Dynamic Simulation implementation for the Flare System Design 107

7.1. Proper Design Stage for the Estimation of the Relief Load 107

7.2. Cost Effect of the Dynamic Simulation.....110

8. Conclusion 117

References.....120

LIST OF TABLES

Table 1.1 Typical relief scenarios and a corresponding estimation method for relief capacities 5

Table 2.1 Target probability on demand for each safety integrity level.....20

Table 2.2 Probability of failure on demand for pressure safety valve.....20

Table 2.3 Terms used in FTA 28

Table 2.4 Rules for fault tree calculation.....31

Table 2.5 Selected rules of Boolean algebra 31

Table 3.1 Relief scenarios and its effects for the ethane separation system 38

Table 3.2 Stream data for the ethane separation system.....41

Table 3.3 The relief load calculation for the reflux failure scenario of the ethane separation system (Normal Condition) 42

Table 3.4 The relief load calculation for the reflux failure scenario of the ethane separation system (Abnormal Condition)..43

Table 3.5 The relief load calculation results for the ethane separation system by using the heat and material balance method.....44

Table 3.6 The relief load calculation results for the butane separation system by using the heat and material balance method.....46

Table 3.7 The relief load calculation results for the isopentane separation system by using the heat and material balance method.....47

Table 3.8 All events which can be happened during the general power failure for the liquid fractionation unit 49

Table 3.9 The relief load calculation for the general power failure scenario of the ethane separation system.....50

Table 3.10 The relief load calculation for the general power failure scenario of the butane separation system 51

Table 3.11 The relief load calculation for the general power failure scenario of the isopentane separation system.....52

Table 3.12 Stream data for the 1st xylene splitter 58

Table 3.13 The relief load estimation results for the 1st xylene splitter by using the heat and material balance method..59

Table 3.14 The relief load estimation results for the 2nd xylene splitter by using the heat and material balance method..60

Table 3.15 The relief load estimation results for the 1st column in the PAREX unit by using the heat and material balance method.....61

Table 3.16 The relief load estimation results for the 2nd column in the PAREX unit by using the heat and material balance method.....62

Table 3.17 All events which can be happened during the general power failure for the xylene fractionation and the PAREX unit 64

Table 3.18 The relief load calculation for the general power failure scenario of the xylene fractionation and the PAREX unit.....65

Table 4.1 Equipment data of the ethane separation system.....68

Table 4.2 Equipment data of the butane separation system 69

Table 4.3 Equipment data of the isopentane separation system.....70

Table 4.4 Typical Ranges of Control Parameters 71

Table 4.5 Dynamic simulation results of the relief load estimation for the butane separation system and the isopentane separation system 76

Table 4.6 Dynamic simulation results summary for the liquid fractionation unit.....81

Table 4.7 Relief load estimation results by using a dynamic simulator for the 1st xylene splitter 83

Table 4.8 Relief load estimation results by using a dynamic simulator for the 2nd xylene splitter 84

Table 4.9 Relief load estimation results by using a dynamic simulator for the 1st column in the PAREX unit 85

Table 4.10 Relief load estimation results by using a dynamic simulator for the 2nd column in the PAREX unit 86

Table 4.11 Dynamic simulation results summary for the xylene fractionation and the PAREX unit 92

Table 5.1 Governing relief cases and corresponding relief loads of the liquid fractionation unit 94

Table 5.2 Governing relief cases and corresponding relief loads of the xylene fractionation and the PAREX unit 96

Table 7.1 Reduction rates of the relief load in the dynamic simulation..... 111

Table 7.2 Results of preliminary flare header design and its estimated material cost 112

Table 7.3 Results of simplified HIPS configuration by combining HIPS and the dynamic simulation..... 114

Table 7.4 Characteristics of Relief Load Estimation Method..... 115

LIST OF FIGURES

Figure 1.1 The diagram for layers of protection.....3

Figure 2.1 The design procedure for the flare system 10

Figure 3.1 The process flow diagram of the liquid fractionation unit 33

Figure 3.2 The block diagram of the liquid fractionation unit.....33

Figure 3.3 The simple drawing of the ethane separation unit 37

Figure 3.4 The PFD of the xylene fractionation and the PAREX unit 55

Figure 4.1 The overall event flow of the reflux failure scenario for the ethane separation system 73

Figure 4.2 Dynamic simulation result of the reflux failure scenario for the ethane separation system 74

Figure 4.3 Dynamic simulation result of the condenser duty loss scenario for the ethane separation system.....74

Figure 4.4 Dynamic simulation result of the abnormal heat input scenario for the ethane separation system.....75

Figure 4.5 Stabilization result of the liquid fractionation unit.....78

Figure 4.6 Dynamic simulation result for the ethane separation unit when the general power failure happened (320.92 ton/hr) 78

Figure 4.7 Dynamic simulation result for the butane separation unit when the general power failure happened (59.69 ton/hr) 79

Figure 4.8 Dynamic simulation result for the isopentane separation unit when the general power failure happened (0 ton/hr) 79

Figure 4.9 Stabilization results of the xylene fractionation and the PAREX unit.....88

Figure 4.10 Dynamic simulation result for the 1st xylene splitter when the general power failure happened.....88

Figure 4.11 Dynamic simulation result for the 2nd xylene splitter when the general power failure happened.....89

Figure 4.12 Dynamic simulation result for the 1st column in the PAREX unit when the general power failure happened.....89

Figure 4.13 Dynamic simulation result for the 2nd column in the PAREX unit when the general power failure happened.....90

Figure 6.1 HIPS configuration for the ethane separation system.....101

Figure 6.2 HIPS configuration for the butane and isopentane separation system.....101

Figure 6.3 Dynamic simulation result for the ethane separation unit when HIPS implemented in the ethane separation system only 103

Figure 6.4 Dynamic simulation result for the butane separation unit when HIPS implemented in the ethane separation system only 104

Figure 6.5 Dynamic simulation result for the isopentane separation unit when HIPS implemented in the ethane separation system only 104

Figure 6.6 Result of FTA analysis.....106

Figure 7.1 Design steps of a plant design.....109

Figure 7.2 New Design Procedure for the Efficient Flare System Design.....109

1. Introduction

The objective of chemical engineering is to create new material wealth via various chemical interactions between materials [1]. Among various engineering, chemical process engineering is the innovative application of academic theories to design various chemical plants. And these plants are the combined effort of lots of engineers who participates in a design stage of plants. In addition, a construction of plants is a time-consuming and highly expensive task.

However, chemical plants are always confronted with lots of risky problems since chemical plants often handle highly explosive or highly toxic or highly corrosive or highly reactive materials. Therefore, process engineers are always pay attention to the safety of the plant. Consequently, there are lots of devices such as a controller, a safety instrumented system (SIS), a physical protection system and etc., which can protect a plant from various abnormal events. These devices or systems are so called the layers of protection and shown in Figure 1.1.

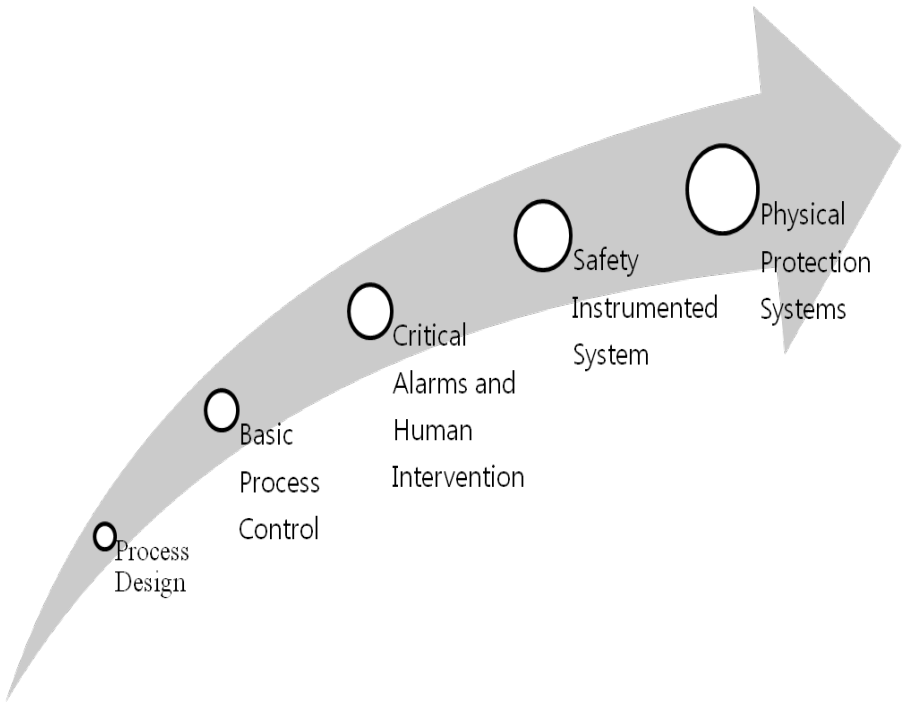

Figure 1.1 The diagram for layers of protection

Especially, the flare system is the most common physical protection system in order to protect a plant from various overpressure events. According to American Petroleum Institute (API) STD 521, “Guide for Pressure-Relieving and Depressuring Systems”, flare is device or system used to safely dispose of relief gases in an environmentally compliant manner through the use of combustion [2]. Like this definition, the flare system prevents a catastrophic accident from an overpressure event as relieving gases or liquids from the over-pressurized system through various relieving devices such as a pressure relief valve, a rupture disc and a blow down valve [32, 46]. The flare system is usually consists of pressure relief devices, flare headers (pipelines), flare knock out drums and flare stacks including burners etc.

The flare system shall be sized for the maximum simultaneous relief load from multiple relief valves or the single relief load from the single relief valve, which is biggest [33]. In order to size whole flare system properly, a reasonable relief load should be calculated. The relief load is important since it will affect the size of overall flare system. If we overestimate the relief load, we waste our resources since the flare system is usually a huge and costly system which operates only when overpressure events occur. On the other hand, if we underestimate the relief load, we will be confronted with a

difficulty since the flare system cannot relieve the pressure from the over-pressurized system.

Therefore, the relief load estimation method is a very crucial issue in industry and there have been several studies regarding this issue. API sets up basic guidelines for sizing relief devices and estimation method for relief loads [2~4]. Especially, API lists several typical relief scenarios and a corresponding estimation method for relief capacities [2] and it is summarized in Table 1.1.

Although API suggests basic guidelines and has tried to standardize calculation method of relief loads, there is much room for interpretation and there is no a consistent procedure to calculate relief loads accurately. Therefore, the heat and material balance method is widely used for estimating relief loads according to API guidelines in industry since it provides the specific means to calculate relief loads. However, the heat and material balance method tends to overestimate relief loads. In order to overcome these problems, J. R. Cassata, S. Dasgupta, and S. L. Gandhi adopted the dynamic simulation for the study of tower relief in order to avoid over-sizing and overestimation of the flare system [5]. They successfully proved that the dynamic simulation was able to accurately quantify the maximum relief load and time dependency of the relief load.

Table 1.1 Typical relief scenarios and a corresponding estimation method for relief capacities [2]

Relief Scenario	Estimation Method for Relief Capacities
Cooling Water Failure to Condenser	Total vapor to condenser at relieving Conditions.
Air-cooled exchangers	Fan failure; size valves for the difference between normal and emergency duty.
Partial Power Failure	One distribution centre, one motor control centre, or one bus is affected
General Power Failure	All electrically operated equipment is simultaneously affected.
Closed Outlets on Vessels	Total incoming steam and vapor plus that generated therein at relieving conditions.
Top-tower reflux failure	Total incoming steam and vapor plus that generated therein at relieving conditions less vapor condensed by side stream reflux.

V. Patel et al., also illustrated that the dynamic simulation could be beneficially used for precise analysis of the peak relief loads for the ethylene plant [6]. In this study, they suggested that the dynamic simulation can be used for the evaluation of the optimum location of High Integrity Protection Systems (HIPS). HIPS are systems which require high Safety Instrumented System (SIS) safety availability and it can be used for the relief load mitigation. A.E. Summers insisted that HIPS can be used to provide overpressure protection if a quantitative or qualitative risk analysis of the proposed system is made addressing credible overpressure scenarios and the process dynamics are evaluated to ensure that the HIPS response is fast enough to prevent overpressure events [7].

According to several studies which are referred above, the dynamic simulation can be used for the accurate relief load estimation and HIPS are able to be used for the mitigation of relief load if the process dynamics are evaluated. However, the dynamic simulation has a big problem to estimate flare loads of whole plant since it will be an extremely time-consuming work if we try to simulate whole plant by using a dynamic simulator.

As previous stated, the existing relief load estimation method which are based on API standards and the heat and material balance method is proved, fast and logical method but too conservative. On the other

hand, the new relief load estimation method which is based on process dynamics is expected to give a rigorous result but it is time-consuming and not proved yet.

Therefore, the new design procedure in order to estimate rigorous relief loads are needed for the efficient flare system design by combining the existing method which is based on codes and the new method which is based on performance. In this paper, two case studies regarding the relief load estimation for column systems will be illustrated in order to compare results between the existing relief load estimation method and the new relief load estimation method. In addition, the relief load mitigation method which combines HIPS and the dynamic simulator also will be presented. And then, the new design procedure for the efficient flare system will be suggested. The procedure developed in this article is the general application to a design of any flare system for columns that can be simulated by using a process simulator.

This thesis is organized as follows.

In chapter 2, background theories of this research including the key concepts of the relief load estimation by using the heat and material balance method and the dynamic simulator will be presented. In addition, basic theories regarding high integrity protection systems also will be introduced.

In chapter 3, the detailed procedure of the relief load estimation method by using the heat and the material balance will be presented. Two detailed examples such as the liquid fractionation unit and the xylene fractionation and the PAREX unit will be also illustrated.

In chapter 4, the detailed procedure of the relief load estimation method by using a dynamic simulator will be presented. Two detailed examples as stated earlier will be also illustrated.

In chapter 5, results of the relief load estimation will be analyzed and discussed. Through this analysis and discussion, the reason why the dynamic simulation gives more rigorous results for the relief load estimation than the heat and the material balance method will be clarified.

In chapter 6, the relief load mitigation method using HIPS and the dynamic simulator will be illustrated. The effect of a combination between HIPS and the dynamic simulator will be investigated.

In chapter 7, the effect of the dynamic simulation implementation for the flare system design will be analyzed. The proper design stage in order to implement the dynamic simulation for the relief load estimation and the cost effect of implementing the dynamic simulation will be presented. Finally, the new design procedure for the flare system design will be suggested.

In chapter 8, conclusions of this research will be presented.

2. Background Theories

As previous stated, the exact relief load calculation is very important in order to design whole flare system properly. D. A. Crowl and J. F. Louvar suggest an overall design procedure for the flare system [8] and it is shown in Figure 2.1. As shown in Figure 2.1, a process engineer has to determine the location of pressure relief devices and then, develop possible scenarios which can cause overpressure events [40-45] in order to calculate relief loads. In this research, possible scenarios which can cause overpressure events were evaluated according to API STD 521 and relief loads for evaluated scenarios were calculated using both the heat and material balance method and the dynamic simulator for the comparison purpose. Determining the location of pressure relief devices is beyond the scope of this research.

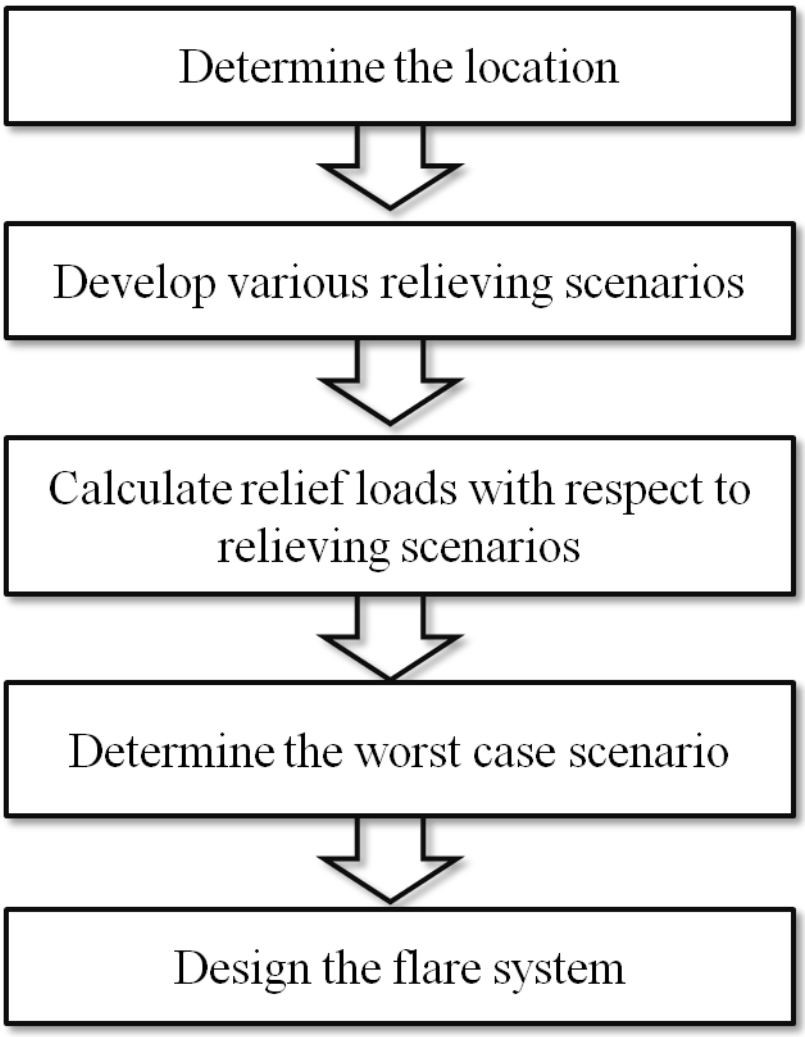

Figure 2.1 The design procedure for the flare system

2.1. Relief Load Estimation by Using the Heat and Material Balance Method

In industry, the heat and material method is often employed in order to calculate a relief load and this is based chiefly on equilibrium condition during the relieving. In this method, a mass accumulation is calculated by Equations 2.1 and 2.2.

$$\sum W_F = \sum W_P \qquad (2.1)$$

$$W_A = \frac{(\sum W_F H_F + \sum Q_I) - (\sum W_P H_P + \sum Q_O)}{L_A} \qquad (2.2)$$

Where H_F Enthalpy of feed stream (kcal/hr)

H_P Enthalpy of product stream (kcal/hr)

L_A Latent heat of accumulated fluid

Q_I Heat Input (kcal/hr)

Q_O Heat Output (kcal/hr)

W_A Accumulated mass flow (kg/hr)

W_F Mass flow of feed stream (kg/hr)

W_P Mass flow of product stream (kg/hr)

This method is quite easy to understand and provides the specific means to calculate the relief load. Therefore, this method may be suitable for the preliminary design of the flare system. However, the heat and material balance method has several inherent limitations since it is based on a steady state, whereas an overpressure event is a function of lots of variables such as time, heat input rate, heat output rate, liquid holdup and etc. For example, the heat and material balance method does not account for the effects of controllers and the dynamic changes of system conditions which may cause changes in properties of process fluid such as the latent heat of relieving fluid. In addition, this method ignores the dynamic interaction between units or equipments. Therefore, more accurate estimation is needed for optimization of the whole flare system although the heat and material balance method is suitable in the initial design and sizing of the flare system.

2.2. Dynamic Simulator

2.2.1. General Descriptions

Dynamic simulation has come into the spotlight as processes become more complex and are designed and operated closer to constraints [9, 30]. Dynamic simulation has great advantages when process engineers want to see what is going to be happened in the process during the transition state such as start up, emergency shout down and overpressure events.

The use of a commercial steady-state process simulator has proven to be a useful tool for the design and optimization of chemical processes. However, chemical plants are never truly at steady state due to feed and environmental disturbances, heat exchanger fouling, catalytic degradation and etc [10]. Therefore, chemical engineers always should do the study of both steady state and dynamic behavior of chemical processes whenever they design and optimize a chemical plant. Chemical engineers can check steady state energy balance and material balances, and evaluate different plant scenarios by using a steady state simulator. By doing so, chemical engineers can optimize the process by reducing capital and equipment costs while maximizing production.

With a dynamic simulator, chemical engineers can confirm that the designed plant can produce the desired product in a safe manner. By defining detailed equipment specifications in the dynamic simulation, chemical engineers can verify that the equipment functions as expected in an actual plant situation. In addition, chemical engineers can find the most suitable control strategies for the designed plant easily by designing and testing a variety of control strategies by using the dynamic simulator.

About 10 years ago, a dynamic simulator has limitations since computing speed is not so fast enough to solve thousands of differential equations which are related to chemical plants. However, the increases in computing speed and the development of several commercial software packages which are able to perform dynamic simulations of chemical plants improve the ability of process engineers to perform dynamic analysis by using a commercial dynamic simulator. As a result, dynamic simulation can be easily performed by chemical engineers at the early stage of the project, nowadays.

Consequently, the relief load estimation by using a dynamic simulator can be applied in the early stage of chemical plant design. As stated earlier, overpressure events which cause the relief are function of various process variables. Therefore, relief load estimation by using a

dynamic simulator can have great advantages since a dynamic simulator can solve thousands of equations involving thousands of variables very quickly.

2.2.2. Mathematical Model in a Dynamic Simulator

Most chemical processes are distributed systems which have thermal or component concentration in three dimensions (x, y, and z) as well as in time. A distributed system can be characterized mathematically by using a set of partial differential equations (PDEs). However, a distributed system is not suitable for the dynamic simulation of chemical processes since solving PDEs is a very rigorous and time consuming work. More simplified system than a distributed system is needed for the dynamic simulation since chemical process contains thousands of process variables.

Ordinary differential equations (ODEs) are used in order to simplify a distributed system since it is much less rigorous than PDEs if the x, y, and z gradients are ignored. By doing so, all physical properties of the process are considered to be equal in space and the distributed system is “lumped”.

Consequently, only the time gradients are considered in an analysis of the process. The lumped system is very useful for a dynamic simulator since a dynamic simulator can save calculation time by using the lumped system in a dynamic simulation. For most instances, solving ODEs for the lumped system gives a reasonable solution for the distributed model.

A linear first-order ODE can be describes by Equation 2.3 [39].

$$\tau Y' + Y = Kf(u) \quad (2.3)$$

In a non-linear equation, the process variable Y has a non-linear relationship with other process variables such as a power, exponential and independent. One example of a non-linear equation is shown in Equation 2.4.

$$\tau Y' + Y^3 = Kf(u) \quad (2.4)$$

The most of chemical engineering processes are nonlinear since non-linearity comes from equations describing reaction rates of chemical systems, equilibrium behavior and fluid flow behavior.

Although there are several methods in order to solve ODEs, Hysys which is the dynamic simulator used in this research, adopt an Implicit Euler method. Implicit Euler method can be expressed by Equation 2.5.

$$Y_{n+1} = Y_n + \int_{t_n}^{t_{n+1}} Y' dt \quad (2.5)$$

The Implicit Euler method is simply an approximation of Yn+1 using rectangular integration.

2.3. High Integrity Protection Systems (HIPS)

2.3.1. General Descriptions

High Integrity Protection Systems (HIPS) is an instrumented safety system which is designed and built in accordance with related codes and standards [11 - 19]. HIPS are different approaches to overpressure protection by using a high reliable instrumented system instead of using a traditional physical protection device such as a pressure relief valve [31]. According to API STD 521, HIPS can replace the PRV if HIPS are designed to achieve a level of availability equal to or greater than a mechanical relief device. Generally, HIPS have complete functional loops which consist of sensors, logic solvers and final elements and satisfies the safety integrity level (SIL) 3 at least. Therefore, HIPS can be used as the protection device instead of the pressure relief valve (PRV) since the probability of failure on demand (PFD) of PRV lies between SIL 2 and SIL 3 [20 - 21]. Target PFD for each safety integrity level are shown in Table 2.1 and PFD for each pressure relief valve are shown in Table 2.2.

Table 2.1 Target probability on demand for each safety integrity level

Safety Integrity Level (SIL)	Target Probability on Demand (PFD)	Target Availability (1-PFD)
1	0.1 to 0.01	0.9 to 0.99
2	0.01 to 0.001	0.99 to 0.999
3	0.001 to 0.0001	0.999 to 0.9999
4	0.0001 to 0.00001	0.9999 to 0.99999

Table 2.2 Probability of failure on demand for pressure safety valve

PFD	Type of Pressure Safety Valve
$4.15 * 10^{-3}$	Pilot operated
$2.12 * 10^{-4}$	Spring operated
$3.20 * 10^{-3}$	General PRV

However, the implementation of HIPS should be decided with a great deal of caution and careful consideration since the application of HIPS requires particular attention during its operational life such as maintenance, testing and inspection. Nevertheless, HIPS are very attractive to process engineers since it is cost-effective system. By eliminating the need for costly upgrades to an existing flare system or by reducing the size of a new flare system, a large amount of capital savings can be achieved.

API STD 521 lists five principal uses of HIPS as follows:

1) To eliminate a particular overpressure scenario form the design basis.
2) To eliminate the need for a particular relief device.
3) To provide system overpressure protection where a relief device is ineffective
4) To reduce the probability that several relief devices will have to operate simultaneously, thereby allowing for a reduction in the size of the disposal system.
5) To reduce the demand rate on a relief device consequently reducing the risk.

As referred above, HIPS can coexist with PRV when HIPS are used to reduce the relief load as eliminating the scenario which causes the maximum relief load or particular relief devices.

2.3.2. Calculation Method of Probability of Failure on Demand (PFD) of HIPS

Generally, HIPS consist of three sub systems such as the sensor subsystem, the logic subsystem and the final element subsystem [38]. Therefore, the average PFD of HIPS is determined by calculating and combining the average PFD for all the subsystems which together execute the safety function. This can be calculated by Equation 2.6.

$$\mathrm{PFD_{SYS}} = \mathrm{PFD_S} + \mathrm{PFD_L} + \mathrm{PFD_{FE}} \quad (2.6)$$

Where $\mathrm{PFD_{SYS}}$: average PFD for HIPS

$\mathrm{PFD_S}$: average PFD for the sensor subsystem

$\mathrm{PFD_L}$: average PFD for the logic subsystem

$\mathrm{PFD_{FE}}$: average PFD for the final element subsystem

In order to determine the average PFD for each of the subsystem, the following equations are used [11-19].

2.3.2.1. 1 Out of 1 System

This architecture is made up of a single channel, where any dangerous failure leads to a failure of the HIPS when a demand arises. The dangerous failure rate for the channel is given by Equations 2.7 to 2.9.

$$\lambda_D = \lambda_{DU} + \lambda_{DD} \quad (2.7)$$

Where λ_D : dangerous failure rate (per hour) of a channel in a subsystem

λ_{DU} : undetected dangerous failure rate (per hour) of a channel in a subsystem

λ_{DD} : detected dangerous failure rate (per hour) of a channel in a subsystem

$$t_{CE} = \frac{\lambda_{DU}}{\lambda_D}\left(\frac{T_1}{2} + MRT\right) + \frac{\lambda_{DD}}{\lambda_D} MTTR \quad (2.8)$$

Where t_{CE} : channel equivalent mean down time (hour)

T_1 : proof test interval (hour)

MRT : Mean Repair Time (hour)

MTTR : Mean Time to Restoration (hour)

$$PFD = (\lambda_{DU} + \lambda_{DD})t_{CE} \quad (2.9)$$

2.3.2.2. 1 Out of 2 System

This architecture is made up of two parallel channels, such that either channel can process the safety function. A dangerous failure in any channel leads to a failure of the HIPS when a demand arises. The average PFD for this system can be calculated by Equations 2.10 to 2.11.

$$t_{GE} = \frac{\lambda_{DU}}{\lambda_D}\left(\frac{T_1}{3} + MRT\right) + \frac{\lambda_{DD}}{\lambda_D}\ MTTR \quad (2.10)$$

Where t_{GE} : voted group equivalent mean down time (hour)

$$PFD = 2\left((1-\beta)\lambda_{DU} + (1-\beta_D)\lambda_{DD}\right)^2 t_{CE} t_{GE} + \beta_D \lambda_{DD} MTTR + \beta\lambda_{DU}\left(\frac{T_1}{2} + MRT\right) \quad (2.11)$$

Where β : the fraction of undetected failures

β_D : Of those failures that are detected by the diagnostic tests

2.3.2.3. 2 Out of 2 System

This architecture is made up of two parallel channels so that both channels need to demand the safety function before it can take place. The average PFD for this system can be calculated by Equation 2.12.

$$\mathrm{PFD} = \lambda_{\mathrm{D}} t_{\mathrm{CE}} \qquad (2.12)$$

2.3.2.4. 2 Out of 3 System

This architecture is made up of three parallel channels so that two channels need to demand the safety function before it can take place. The average PFD for this system can be calculated by Equation 2.13.

$$\begin{aligned}\mathrm{PFD} = 6\big((1-\beta)\lambda_{\mathrm{DU}} + (1-\beta_{\mathrm{D}})\lambda_{\mathrm{DD}}\big)^2 t_{\mathrm{CE}} t_{\mathrm{GE}} \\ + \quad \beta_{\mathrm{D}}\lambda_{\mathrm{DD}}\mathrm{MTTR} \\ + \beta\lambda_{\mathrm{DU}}\left(\frac{T_1}{2} + \mathrm{MRT}\right) \qquad (2.13)\end{aligned}$$

2.4. Fault Tree Analysis (FTA)

2.4. 1. General Description

Fault tree analysis is useful method in order to determine the probability of a safety accident and it is often used in the field of safety engineering or reliability engineering [37]. Fault Trees were first developed at Bell Telephone Laboratories in 1961 for missile launch control reliability [22]. D. F. Haasl further developed the technique at Boeing [23]. It has been an essential part of nuclear safety analysis since 1975 [24]. Nowadays, fault trees are finding greater application in the chemical process industry.

Fault Tree Analysis (FTA) provides a structured method for determining the causes of an incident [25]. The fault tree represents the various interrelationships of equipment failures than can cause incidents. This is a deductive method which can determine causes of certain accident event and provide powerful qualitative insight into the potential failures. The undesired event appears as the top event and the trees are drawn from top to bottom. Two basic logic gates connect event blocks: the And-gate and the OR-gate. Terms used in FTA are summarized in Table 2.3.

Table 2.3 Terms used in FTA [22]

Term	Definition
Event	An unwanted deviation from the normal or expected sate of a system component
Top event	The unwanted event or incident at the "top" of the fault tree that is traced downward to more basic failures using logic gates to determine its causes and likelihood
Intermediate event	An event propagates or mitigates an initiating (basic) event during the accident sequence
Basic event	A fault event that is sufficiently basic that no further development is judged necessary
Logic gate	A logical relationship between input events and a single output event. These logical relationships are normally represented as AND or OR gates

The Center for Chemical Process Safety (CCPS) suggests the stepwise procedure for implementing FTA as follows [22]:

1) System description and choice of system boundary
2) Hazard identification and selection of the top event
3) Construction of the fault tree
4) Qualitative examination of structure
5) Quantitative evaluation of the fault tree

The top event frequency or probability can be calculated by using the minimal cut set approach if the final structure of a fault tree and estimated probability or frequency is given.

2.4. 2. Minimal Cut Set Approach

Minimal cut set approach is a useful mathematical method for calculating the top event frequency or probability. The basic event combinations which consist of the top event, called cut sets are reduced to identify minimal cut sets, which contain the minimum sets of events necessary and sufficient to cause of the top event.

If it is too difficult to calculate the top event frequency or probability since the fault tree is too big and complex, the fault tree can be mathematically transformed into an equivalent minimal cut set tree which is simpler than the fault tree by using the rules of Boolean algebra. Rules for fault tree calculation and selected rules of Boolean algebra are summarized in Tables 2.4 and 2.5.

Table 2.4 Rules for fault tree calculation [22]

Gate	Input pairing	Calculation for output
OR	P_A OR P_B	P(A OR B) = 1-(1-P_A)(1-P_B)
	F_A OR F_B	F(A OR B) = F_A + F_B
	P_A OR F_B	Not permitted
AND	P_A AND P_B	P(A AND B) = $P_A P_B$
	F_A AND F_B	Unusual pairing, reform to F_A AND P_B
	F_A AND P_B	F(A AND B) = $F_A P_B$

a. P, probability; F, frequency

Table 2.5 Selected rules of Boolean algebra [22]

Rule	Mathematical form
Commutative Rule	A·B = B·A A+B = B+A
Associative Rule	A·(B·C) = (A·B)·C A+(B+C) = (A+B)+C
Distributive Rule	A·(B+ C)= A·B+ A·C A+(B·C) = (A+B)·(A+C)
Idempotent Rule	A·A = A A+A = A
Rule of Absorption	A·(A+ B)= A A+A·B = A

3. Relief Load Estimation by Using the Heat and Material Balance Method

3.1. Relief Load Estimation for the Liquid Fractionation Unit

In this section, the liquid fractionation unit will be analyzed in order to estimate relief loads from towers. Generally, the liquid fractionation unit is located after the cryogenic unit which includes a demethanizer and a turbo-expander in a gas separation plant. The primary purpose of the liquid fractionation unit is saving resources as recovering useful products from the waste liquid of the cryogenic unit. The liquid fractionation unit can have various combinations with respect to desired products. In this research, the liquid fractionation unit which has three towers such as a deethanizer, a debutanizer and a deisopentanizer is presented and showed in Figures 3.1 to 3.2.

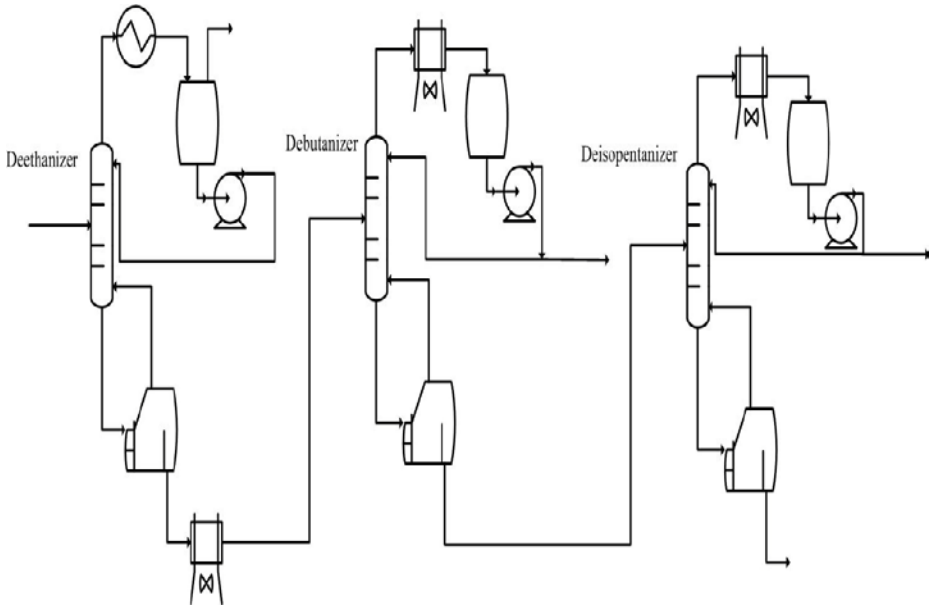

Figure 3.1 The process flow diagram of the liquid fractionation unit

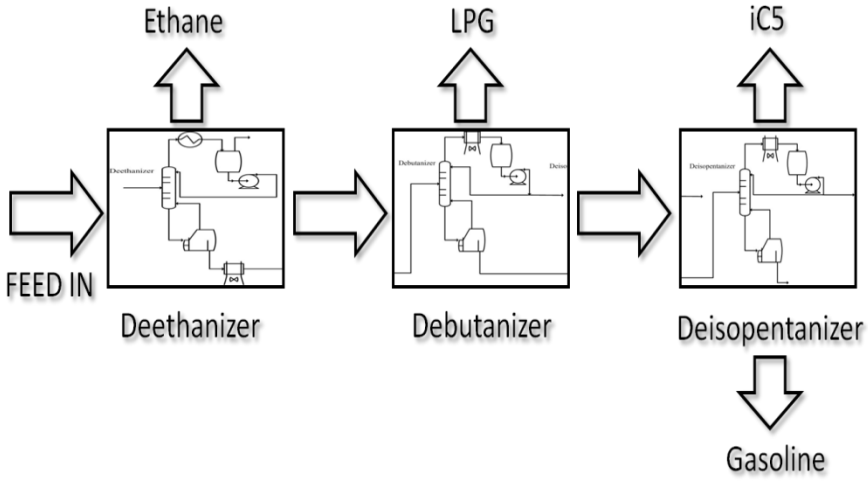

Figure 3.2 The block diagram of the liquid fractionation unit

The feed stream which comes from the cryogenic unit has lots of ethane and ethane is recovered from the top of the deethanizer. The minimum recovery ratio of ethane is 98 mol %. The condenser cold source of the deethanizer is the propane which comes from the propane refrigeration system and the heat source of the deethanizer is the low pressure steam (LP steam). The ethane product is compressed and transferred to the outside battery limit (OSBL). The liquid product from the deethanizer is cooled by the air fin cooler and then goes to the next tower, debutanizer.

Debutanizer column recovers Liquefied Petroleum Gas (LPG) from the top and the required purity of LPG product is min. 96 mol % of C3 and C4 in this case. The condensing duty is provided by the air fin cooler and the heat duty is provided by the medium pressure steam. The LPG product is pumped to the LPG storage tank.

The last column is the deisopentanizer. This column recovers isopentane from the top and gasoline from the bottom. The required purity of isopentane product is min. 96 mole % of i-C5. The condensing duty is provided by the air fin cooler and the heat duty is provided by the low pressure steam. Both products are pumped to corresponding storage tanks.

The liquid fractionation unit is relatively simple since it does not have any heat integrated system. Therefore, it is a valuable example to

conduct a comparison of results of relief load estimation between the heat and material balance method and the dynamic simulation method.

3.1.1. Relief Load Estimation from a Single Source

In order to estimate the relief load, the development of relief scenarios should be preceded. For the sake of convenience, the liquid fractionation unit was divided into 3 sections such as the ethane separation section, the butane separation section and the isopentane separation section.

First of all, the ethane separation section was analyzed and the simple drawing of the ethane separation section is shown in Figure 3.3. Possible relieving scenarios and its effects for the ethane separation system were developed according to API RP 521 and summarized in Table 3.1. The external fire case is not included in this research since external fire case does not determine the maximum relief load of columns, generally.

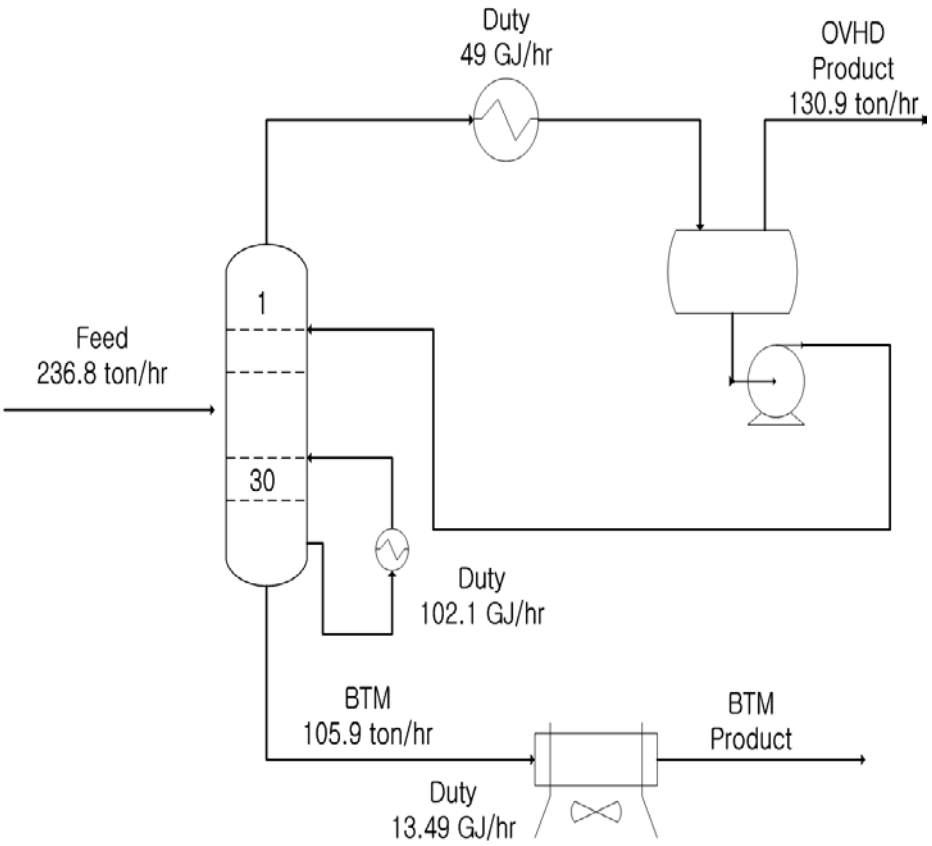

Figure 3.3 The simple drawing of the ethane separation unit

Table 3.1 Relief scenarios and its effects for the ethane separation system

Relief Scenario	Effects on the Ethane Separation System
Condenser Duty Loss	1. Condenser duty may be lost due to the C3-refrigerant pump Failure. 2. If condenser duty loss happens, the level of the overhead receiver will go down and the reflux pump will stop. 3. Consequently, reflux will stop and the pressure of the deethanizer will go up.
Reflux Failure	1. Reflux failure may happen due to the reflux pump failure. 2. If reflux failure happens, the overhead receiver will be flooding. 3. Then, the overhead condenser will lose its duty and no more overhead products will be produced. 4. Consequently, the pressure of the deethanizer will go up.
Partial Power Failure	1. Partial Power may happen due to various reasons. 2. If Partial power failure happens, the reflux pump and the air fin cooler will stop. 3. The failure of the air fin cooler does not effect on the pressure of the ethanizer.

	4. Consequently, effects of Partial power failure are totally same as reflux failure.
Closed Outlets on the overhead receiver	1. Closed outlets on the overhead receiver may happen due to control valves failure. 2. If closed outlets on the overhead receiver happen, reflux will fail and no more overhead products will be produced. 3. Consequently, effects of closed outlets on the overhead receiver are totally same as reflux failure.
Abnormal Heat Input	1. Abnormal Heat Input may happen due to full open of the control valve on the LP steam line 2. If abnormal heat input happens, the reboiler will provide excessive heat to the deethanizer. 3. Consequently, the pressure of the deethanizer will go up.

The stream data of feed stream, overhead product stream and bottom product stream are summarized in Table 3.2 and results of the relief load estimation for the reflux failure scenario is summarized in Table s 3.3 and 3.4. Relief pressure of column overhead is 3,600 kPag which is equal to the set pressure of the pressure relief valve and the relief pressure of column bottom is the set pressure of the pressure relief valve plus delta P of the deethanizer. Relief temperature of column overhead is equal to the saturated vapor temperature at 3,600 kPag and relief temperature of column bottom is equal to the saturated liquid temperature at 3,660 kPag. The bottom liquid of the deethanizer was assumed as the relieving fluid and the latent heat of this fluid was used in the calculation of relief load. All these parameters were calculated by using HYSYS 7.3. Other scenarios were analyzed same way and results are summarized in Table 3.5. As a result, the reflux failure scenario caused the maximum relief load in this case.

Table 3.2 Stream data for the ethane separation system

Stream Name	Temp. (deg C)	Pressure (kPag)	Mass Flow (ton/hr)	Major Component (mole %)
Feed	19.3	3,010	236.8	CO2 : 7.36 C1: 2.11 C2: 57.74 C3: 20.98 C4: 8.82 C5: 2.34
OVHD Product	4	2,950	130.9	CO2 : 11.05 C1: 3.17 C2: 85.75
BTM Product	62	2,960	105.9	C3: 62.87 C4: 26.48 C5: 7.02

Table 3.3 The relief load calculation for the reflux failure scenario of the ethane separation system (Normal Condition)

Normal Condition					
IN					
Stream	**Mass Flow (ton/hr)**	**Temp (deg C)**	**Press (kPag)**	**Mass Enthalpy (kJ/kg)**	**Total Enthalpy (GJ/hr)**
Feed	236.80	19.30	3,010	-3,471.33	-822.01
REB Q					102.10
SUM	236.80				-719.91
OUT					
Stream	**Mass Flow (ton/hr)**	**Temp (deg C)**	**Press (kPag)**	**Mass Enthalpy (kJ/kg)**	**Total Enthalpy (GJ/hr)**
OVHD Product	130.90	4.00	2,950.00	-3,919.90	-513.11
BTM	105.90	99.32	3,060.00	-2,415.50	-255.80
COND Q					49
SUM	236.80				-719.91

Table 3.4 The relief load calculation for the reflux failure scenario of the ethane separation system (Abnormal Condition)

Reflux Failure					
IN					
Stream	**Mass Flow (ton/hr)**	**Temp (deg C)**	**Press (kPag)**	**Mass Enthalpy (kJ/kg)**	**Total Enthalpy (GJ/hr)**
Feed	236.80	19.30	3,600.00	-3,473.00	-822.41
REB Q					102.10
SUM	236.80				-720.31
OUT					
Stream	**Mass Flow (ton/hr)**	**Temp (deg C)**	**Press (kPag)**	**Mass Enthalpy (kJ/kg)**	**Total Enthalpy (GJ/hr)**
OVHD Product	130.90	13.00	3,600.00	-3,927.00	-514.04
BTM	105.90	111.00	3,660.00	-2,364.00	-250.35
COND Q					0.00
SUM	236.80				-764.39
Accumulated Heat	44.09	GJ/hr	Latent Heat of Relieving Fluid	151.30	kJ/kg
Accumulation Rate	291.38	ton/hr	**Relief Load (Accumulation + TOP)**	**422.28**	**ton/hr**

Table 3.5 The relief load calculation results for the ethane separation system by using the heat and material balance method

Relief Scenario	Accumulated Heat (GJ/hr)	Accumulation Rate (ton/hr)	Relieving Fluid	Relieving Rate (ton/hr)
Reflux Failure	44.09	291.38	Accumulation + OVHD Product	422.28
Condenser Duty Loss	44.09	291.38	Accumulation	291.38
Abnormal Heat Input	15.50	102.42	Accumulation	102.42

Same analyses were done for the butane separation system and the isopentane separation system, and results of the relief load calculation are summarized in Tables 3.6 and 3.7. In both systems, the blocked outlets on the vessel scenario and the Partial power failure scenario had a same result. In the case of the butane separation system, the abnormal heat input scenario did not cause the rise of the system pressure at all. As a result, Partial power failure scenario caused the maximum relief load in both systems.

Table 3.6 The relief load calculation results for the butane separation system by using the heat and material balance method

Relief Scenario	Accumulated Heat (GJ/hr)	Accumulation Rate (ton/hr)	Relieving Fluid	Relieving Rate (ton/hr)
Partial Power Failure	14.37	79.32	Accumulation + OVHD Product	173.64
Condenser Duty Loss	2.96	16.32	Accumulation + OVHD Product	110.64
Reflux Failure	14.37	79.32	Accumulation	79.32

Table 3.7 The relief load calculation results for the isopentane separation system by using the heat and material balance method

Relief Scenario	Accumulated Heat (GJ/hr)	Accumulation Rate (ton/hr)	Relieving Fluid	Relieving Rate (ton/hr)
Partial Power Failure	27.72	97.38	Accumulation + OVHD Product	101.60
Condenser Duty Loss	19.64	68.99	Accumulation + OVHD Product	73.21
Reflux Failure	27.72	97.38	Accumulation	97.38
Abnormal Heat Input	1.37	4.80	Accumulation	4.80

3.1.2. Relief Load Estimation from Multiple Sources

In this section, procedure and results of multiple relief load estimation will be presented. Generally, multiple PRV will be opened some scenarios such as general power failure and cooling water failure. In the case of the liquid fractionation unit in this research, general power failure can cause the operation of multiple PRV.

If the general power failure is happened, the feed stream of liquid fractionation unit will stop, all air fin coolers will be lost their duty, all reflux pumps will stop and etc. All events which will be happened are summarized in Table 3.8. The relief load estimation result of the heat and material balance method are summarized in Tables 3.9 to 3.11. Duties of air fin coolers are set to zero since all overhead receivers will be flooding.

Table 3.8 All events which can be happened during the general power failure for the liquid fractionation unit

Object	Possible Events during the General Power Failure
Feed Stream	Flow control valve will be closed during 60 seconds.
Air fin coolers	Air fin coolers will be lost their duty. However, it is assumed that 25 % of normal duty will be continued due to natural convection until the flooding of overhead receivers occurs.
Reflux pumps	All reflux pumps will stop. All reflux streams, butane product stream and isopentane product stream will be cut.
Deethanizer Overhead Condenser	The deethanizer overhead condenser will be lost its duty since the refrigerant compressor will stop.
Ethane Production	Ethane Production will stop since the ethane transportation compressor will be lost its duty.
Reboilers	All reboilers will maintain their duty during 15 minutes.

Table 3.9 The relief load calculation for the general power failure scenario of the ethane separation system

The ethane separation unit					
IN					
Stream	**Mass Flow (ton/hr)**	**Temp (deg C)**	**Press (kPag)**	**Mass Enthalpy (kJ/kg)**	**Total Enthalpy (GJ/hr)**
Feed	0	19.30	3,600.00	-3,473.00	0
REB Q					102.10
SUM	0				102.10
OUT					
Stream	**Mass Flow (ton/hr)**	**Temp (deg C)**	**Press (kPag)**	**Mass Enthalpy (kJ/kg)**	**Total Enthalpy (GJ/hr)**
OVHD Product	0	13.00	3,600.00	-3,927.00	0
BTM	0	111.00	3,660.00	-2,364.00	0
COND Q					0.00
SUM	0				0
Accumulated Heat	102.10	GJ/hr	Latent Heat of Relieving Fluid	151.30	kJ/kg
Accumulation Rate	674.82	ton/hr	**Relief Load (Accumulation)**	**674.82**	**ton/hr**

Table 3.10 The relief load calculation for the general power failure scenario of the butane separation system

The butane separation unit					
IN					
Stream	**Mass Flow (ton/hr)**	**Temp (deg C)**	**Press (kPag)**	**Mass Enthalpy (kJ/kg)**	**Total Enthalpy (GJ/hr)**
Feed	0	62.32	2,100	-2,542.92	0
REB Q					47.00
SUM	0				47.00
OUT					
Stream	**Mass Flow (ton/hr)**	**Temp (deg C)**	**Press (kPag)**	**Mass Enthalpy (kJ/kg)**	**Total Enthalpy (GJ/hr)**
OVHD Product	0	82.75	2,100	-2,268.27	0
BTM	0	179.30	2,150	-1,962.18	0
COND Q					0
SUM	0				0
Accumulated Heat	47.00	GJ/hr	Latent Heat of Relieving Fluid	181.20	kJ/kg
Accumulation Rate	259.38	ton/hr	**Relief Load (Accumulation)**	**259.38**	**ton/hr**

Table 3.11 The relief load calculation for the general power failure scenario of the isopentane separation system

The isopentane separation unit					
IN					
Stream	**Mass Flow (ton/hr)**	**Temp (deg C)**	**Press (kPag)**	**Mass Enthalpy (kJ/kg)**	**Total Enthalpy (GJ/hr)**
Feed	0	98.97	800.00	-2,215.46	0
REB Q					29.85
SUM	0				29.85
OUT					
Stream	**Mass Flow (ton/hr)**	**Temp (deg C)**	**Press (kPag)**	**Mass Enthalpy (kJ/kg)**	**Total Enthalpy (GJ/hr)**
OVHD Product	0	111.29	800.00	-2,004.81	0
BTM	0	140.81	870.00	-2,044.68	0
COND Q					
SUM	0				0
Accumulated Heat	29.85	GJ/hr	Latent Heat of Relieving Fluid	284.61	kJ/kg
Accumulation Rate	104.88	ton/hr	**Relief Load (Accumulation)**	**104.88**	**ton/hr**

3.1.3. Relief Load Estimation Results Summary for a Liquid Fractionation Unit

Relief loads from a single source and multiple sources were calculated for the liquid fractionation unit in this section. As a result, the general power failure scenario caused the maximum relief load for the liquid fractionation system. The total amount of the maximum relief load was 1039.08 ton/hr (674.82 ton/hr + 259.38 ton/hr + 104.88 ton/hr) and this will be the governing load for the liquid fractionation system.

The general power failure scenario also caused the maximum relief load for each individual column. Therefore the governing relief load is 674.82 ton/hr for the ethane separation system, 259.38 ton/hr for the butane separation system and 104.88 ton/hr for the isopentane separation system.

3.2. Relief Load Estimation for the Xylene Fractionation Unit and the PAREX Unit

In this section, the xylene fractionation and the PAREX unit will be analyzed in order to estimate relief loads from towers. The xylene fractionation unit and the PAREX unit is one of the most common units in the petrochemical complex. The purpose of the xylene fractionation unit is the separation of xylenes from the feed and the purpose of the PAREX unit is the production of Para-xylene and toluene.

The xylene fractionation unit and the PAREX unit can have various combinations of columns in real plants. In this research, the xylene fractionation and the PAREX unit consist of 4 separated columns and the PFD for the xylene fractionation and the PAREX unit is presented in Figures 3.4.

The xylene fractionation unit consists of two columns, the 1st xylene splitter and 2nd xylene splitter. Feed streams of two xylene splitters consist of various C6 – C10 hydrocarbons including xylenes. The 1st xylene splitter operates at low pressure, around 7 barg and the 2nd xylene splitter operates at high pressure, around 17 barg.

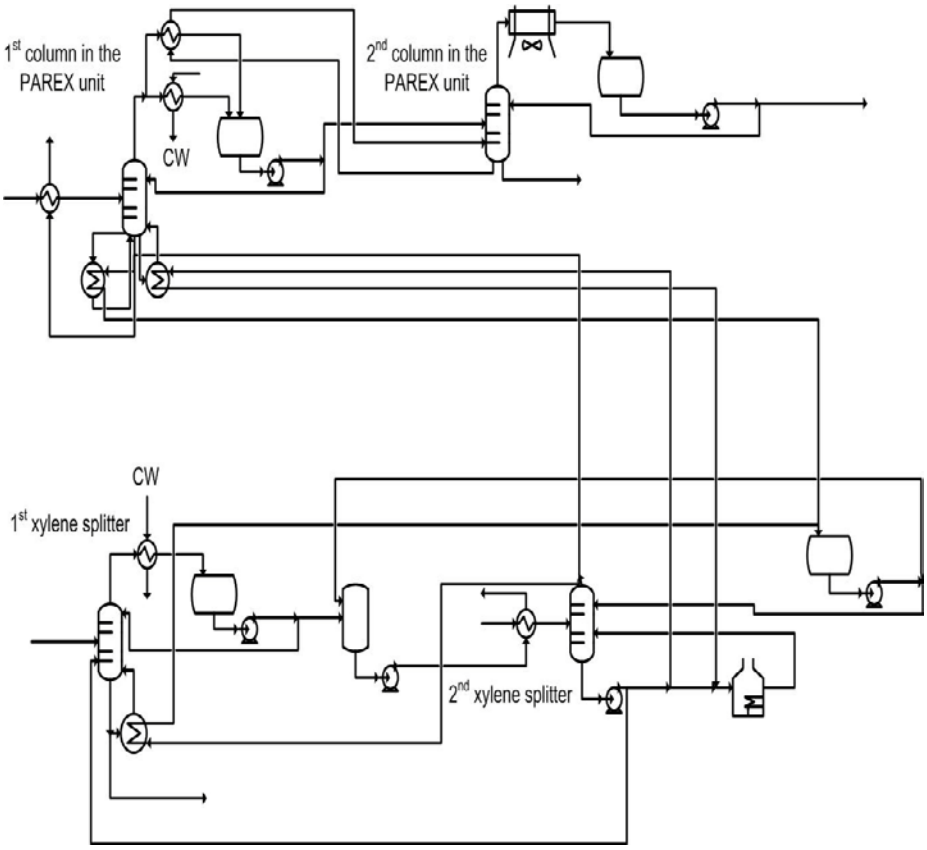

Figure 3.4 The PFD of the xylene fractionation and the PAREX unit

Even though two xylene splitters operate at different pressure, but it produces same products. Ortho, meso and Para xylenes are produced from the top of xylene splitters and heavy hydrocarbons including C9 and C10 aromatics are produced from the bottom of xylene splitters. Produced xylenes go to the PAREX unit via ISOMAR unit. The 1st column in the PAREX unit separates light aromatics including toluene and Para-xylene from the heavy aromatics. Light aromatics go to the 2nd column and it separates toluene as the top product and Para-xylene as the bottom product.

The xylene fractionation unit and the PAREX unit are very difficult to estimate the precise relief load since it is highly heat integrated unit. Since it uses the process stream from other column as a heating or cooling source, we cannot estimate exact heating or cooling duties when overpressure events occur. Therefore, it can be a valuable case study to estimate the exact relief load through the dynamic analysis by using a commercial dynamic simulator.

3.2.1. Relief Load Estimation from a Single Source

In this section, the results of relief load estimation for the xylene fractionation unit and the PAREX unit by using the heat and material balance method will be presented.

First of all, the relief load estimation for the 1st xylene splitter in the xylene fractionation unit was performed. The stream data of the 1st xylene splitter are summarized in Table 3.12. And the result of relief load estimation is summarized in Table 3.13. As a result, the maximum relief load for the 1st xylene splitter is 1080.49 ton/hr and it occurs when the overhead pump failure or overhead receiver blocked outlet happens.

Relief load estimation results for other columns are summarized in Tables 3.14 to 3.16. As a result, the overhead pump failure scenario causes the maximum relief load for all columns. The maximum relief load for the 2nd xylene column, the 1st column in the PAREX unit and the 2nd column in the PAREX unit are 2621.61 ton/hr, 785.39 ton/hr and 211.18 ton/hr respectively.

Table 3.12 Stream data for the 1st xylene splitter

Stream Name	Temp. (deg C)	Pressure (kPag)	Mass Flow (ton/hr)	Major Component (mole %)
Feed 1	187.3	652	242.7	Ethyl BZ : 4.94 o-xylene : 17.13 m-xylene : 29.60 p-xylene : 13.56
Feed 2	162.5	616	64	Toluene : 1.33 Ethyl BZ : 1.62 o-xylene : 21.11 m-xylene : 51.76 p-xylene : 22.71
OVHD Product	219.6	510	214.4	Ethyl BZ : 5.76 o-xylene : 24.70 m-xylene : 47.12 p-xylene : 21.29
BTM Product	274.9	686	92.3	C9 – C10 hydrocarbons and aromatics: 100

Table 3.13 The relief load estimation results for the 1st xylene splitter by using the heat and material balance method

Relief Scenario	Accumulated Heat (GJ/hr)	Accumulation Rate (ton/hr)	Relieving Fluid	Relieving Rate (ton/hr)
Partial Power Failure	107.02	429.29	Accumulation + OVHD product	643.69
Reflux Failure	107.02	429.29	Accumulation	429.29
Cooling Water Failure	107.02	429.29	Accumulation	429.29

Table 3.14 The relief load estimation results for the 2nd xylene splitter by using the heat and material balance method

Relief Scenario	Accumulated Heat (GJ/hr)	Accumulation Rate (ton/hr)	Relieving Fluid	Relieving Rate (ton/hr)
Overhead Pump Failure	221.28	1177.01	Accumulation + OVHD product	1527.76
Reflux Failure	221.28	1177.01	Accumulation	1177.01
1st Condenser Duty Lost	134.67	716.32	Accumulation	716.32
2nd Condenser Duty Lost	4.78	25.41	Accumulation	25.41

Table 3.15 The relief load estimation results for the 1st column in the PAREX unit by using the heat and material balance method

Relief Scenario	Accumulated Heat (GJ/hr)	Accumulation Rate (ton/hr)	Relieving Fluid	Relieving Rate (ton/hr)
Partial Power Failure	95.66	404.13	Accumulation + OVHD product	531.43
Reflux Failure	95.66	404.13	Accumulation	404.13
Cooling Water Failure	24.66	104.18	Accumulation	104.18
Condenser Duty Lost	16.66	70.38	Accumulation	70.38

Table 3.16 The relief load estimation results for the 2nd column in the PAREX unit by using the heat and material balance method

Relief Scenario	Accumulated Heat (GJ/hr)	Accumulation Rate (ton/hr)	Relieving Fluid	Relieving Rate (ton/hr)
Partial Power Failure	60.72	203.21	Accumulation + OVHD product	205.51
Reflux Failure	60.72	203.21	Accumulation	203.21
Air Fin Cooler Failure	60.72	203.21	Accumulation	203.21

3.2.2. Relief Load Estimation from Multiple Sources

In the case of the xylene fractionation and the PAREX unit, the general power failure and the cooling water failure can cause the relief load from multiple relief valves.

In the case of cooling water failure scenario, the relief load can be calculated easily by adding relief loads from the 1st xylene splitter and the 1st column in the PAREX unit. As a result, the relief load when the cooling water failure occurs is 533.47 ton/hr (429.29 ton/hr + 104.18 ton/hr).

If the general power failure is happened, the external feed stream of each column will stop, all air fin coolers will be lost their duty, all pumps will stop, cooling water supply will stop and etc. All events which will be happened are summarized in Table 3.17. The relief load estimation result of the heat and material balance method are summarized in Table 3.18. As you can see in Table 3.18, the total estimated relief load from the xylene fractionation unit and the PAREX unit when the general power failure occurs is 1815.67 ton/hr by using the heat and the material balance method.

Table 3.17 All events which can be happened during the general power failure for the xylene fractionation and the PAREX unit

Object	Possible Events during the General Power Failure
Feed Stream	Flow control valve will be closed during 60 seconds.
Air fin coolers	Air fin coolers will be lost their duty. However, it is assumed that 25 % of normal duty will be continued due to natural convection until the flooding of overhead receivers occurs.
Reflux pumps	All reflux pumps will stop.
Bottom pumps	All bottom pumps for transportation will stop.
Cooling Water Failure	All condensers which use the cooling water as a cooling medium will lose their duty.
Reboilers	All reboilers which use utilities as a heating medium will maintain their duty during 15 minutes.

Table 3.18 The relief load calculation for the general power failure scenario of the xylene fractionation and the PAREX unit

Relief Scenario	Accumulated Heat (GJ/hr)	Relieving Rate (ton/hr)
1st xylene splitter	219.90	882.07
2nd xylene splitter	0.00	0.00
1st column in the PAREX unit	164.36	694.38
2nd column in the PAREX unit	71.48	239.22
TOTAL	**455.74**	**1815.67**

3.2.3. Relief Load Estimation Results Summary for the Xylene Fractionation and the PAREX Unit

Relief loads from a single source and multiple sources were calculated for the xylene fractionation and the PAREX unit in this section. As a result, the general power failure scenario caused the maximum relief load for the xylene fractionation and the PAREX unit. The total amount of the maximum relief load was 1815.67 ton/hr and this will be the governing load for the xylene fractionation and the PAREX unit.

In addition, the general power failure scenario caused the maximum relief load for each individual column except the 2^{nd} xylene splitter. In the case of 2^{nd} xylene splitter, the partial power failure scenario caused the maximum relief load.

4. Relief Load Estimation by Using the Dynamic Simulator

4.1. Relief Load Estimation for a Liquid Fractionation Unit

In this section, procedure and results of dynamic simulation runs in order to estimate the relief load will be presented.

The process flow diagram of the liquid fractionation unit is shown in Figure 3.1. And equipment data which are needed for the dynamic simulation are summarized in Tables 4.1 to 4.3. In addition, control parameters of all controllers must be defined in order to run the dynamic simulation. In this research, all control parameters for each controller were defined within typical ranges of each parameter. Typical ranges of each control parameter are summarized in Table 4.4. [9, 26 – 28, 34, 36, 49, 50] The optimization of control parameters was not carried out since the purpose of this research is not the optimization of control parameters but the estimation of the relief load.

Table 4.1 Equipment data of the ethane separation system

Equipment	Data for the Dynamic Simulation
The Ethane Separation System	
Deethanizer	Tray No. : 30, Dia. : 5.2 m / 6.5 m Reboiler and Sump vol. : 130 m^3 Reboiler Duty : 102.1 GJ/hr Ethane Recovery Ratio : min. 98 mol. % PRV Set Pressure : 3,600 kPag
Overhead Receiver	Vessel Vol. : 96 m^3
Overhead Condenser	Duty : 49 GJ/hr
Bottom Product Air Fin Cooler	Duty : 13.49 GJ/hr

Table 4.2 Equipment data of the butane separation system

Equipment	Data for the Dynamic Simulation
The Ethane Separation System	
Debutanizer	Tray No. : 30, Dia. : 3.8 m Reboiler and Sump vol. : 57 m^3 Reboiler Duty : 47 GJ/hr Butane and Propane mol% in the overhead product : min. 96% PRV Set Pressure : 2,100 kPag
Overhead Receiver	Vessel Vol. : 56 m^3
Overhead Condenser (Air fin cooler)	Duty : 45.6 GJ/hr

Table 4.3 Equipment data of the isopentane separation system

Equipment	Data for the Dynamic Simulation
The Ethane Separation System	
Deisopentanizer	Tray No. : 45, Dia. : 3 m Reboiler and Sump vol. : 35 m3 Reboiler Duty : 29.85 GJ/hr Isopentane mol% in the overhead product : min. 96% PRV Set Pressure : 800 kPag
Overhead Receiver	Vessel Vol. : 27 m3
Overhead Condenser (Air fin cooler)	Duty : 32.3 GJ/hr

Table 4.4 Typical Ranges of Control Parameters

Controller Type	Control Parameter	Ranges
Flow Controller	Proportional Gain	0.3 to 1.5
	Integral (minutes)	0.1 to 1.5
	Derivative	0
Pressure Controller	Proportional Gain	0.6 to 10.0
	Integral (minutes)	1.0 to 50.0
	Derivative	0.0 to 1.5
Temperature Controller	Proportional Gain	0.5 to 5.0
	Integral (minutes)	3 to 20.0
	Derivative	0 to 1.0
Level Controller	Proportional Gain	0.1 to 3.0
	Integral (minutes)	0.5 to 100
	Derivative	0 to 3.0

4.1.1. Relief Load Estimation from a Single Source

The event scheduler in HYSYS was used in order to implement the various overpressure scenarios in the dynamic simulation. For example, the overall event flow of the reflux failure scenario for the ethane separation system is shown in Figure 4.1. All sub events in Figure 4.1 were implemented sequentially by the event scheduler in the dynamic simulation. Like this way, all possible scenarios which can cause an overpressure event were simulated for the ethane separation unit and results are presented in Figures 4.2 to 4.4. Same as the result of the heat and material balance method, the reflux failure scenario caused the maximum relief load for the ethane separation system in the dynamic simulation. However, the amount of the maximum relief load reduced significantly than the result of the heat and material balance method.

All simulation results for other units are summarized in Table 4.5.

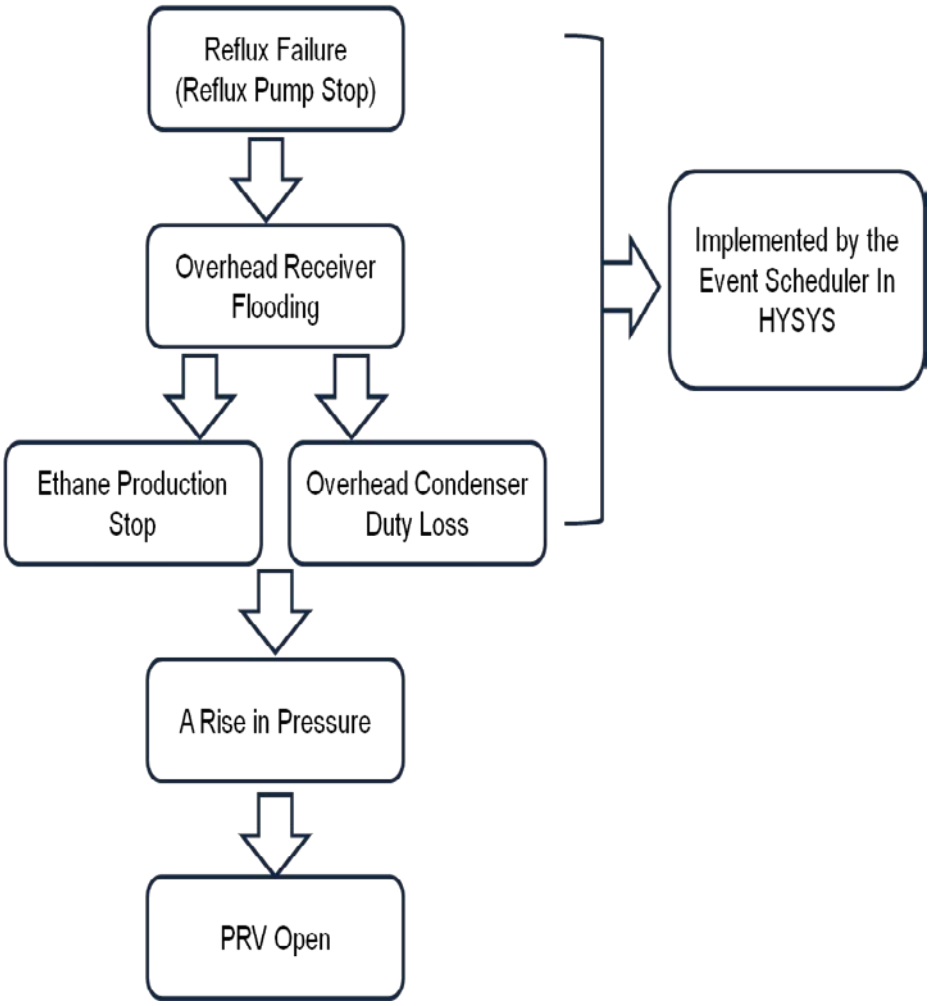

Figure 4.1 The overall event flow of the reflux failure scenario for the ethane separation system

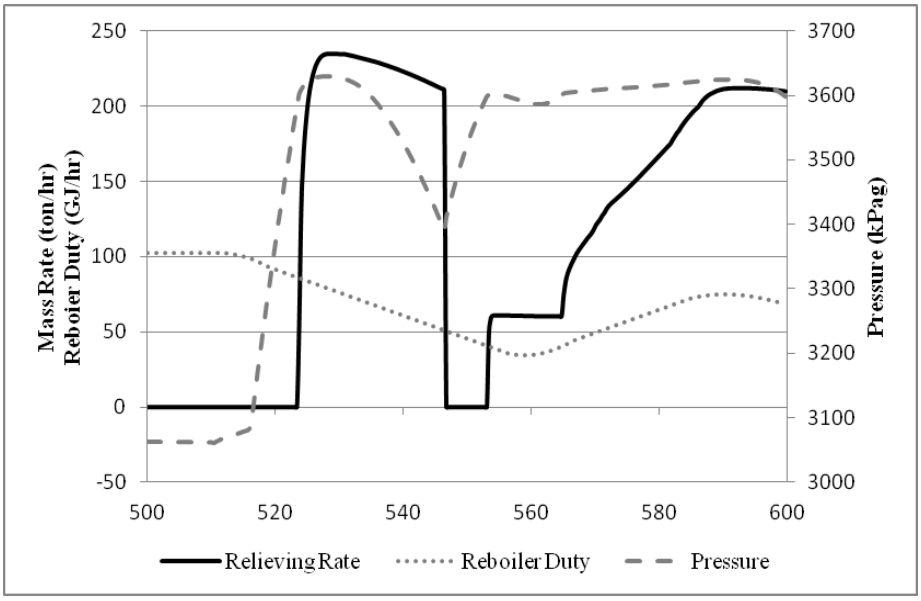

Figure 4.2 Dynamic simulation result of the reflux failure scenario for the ethane separation system

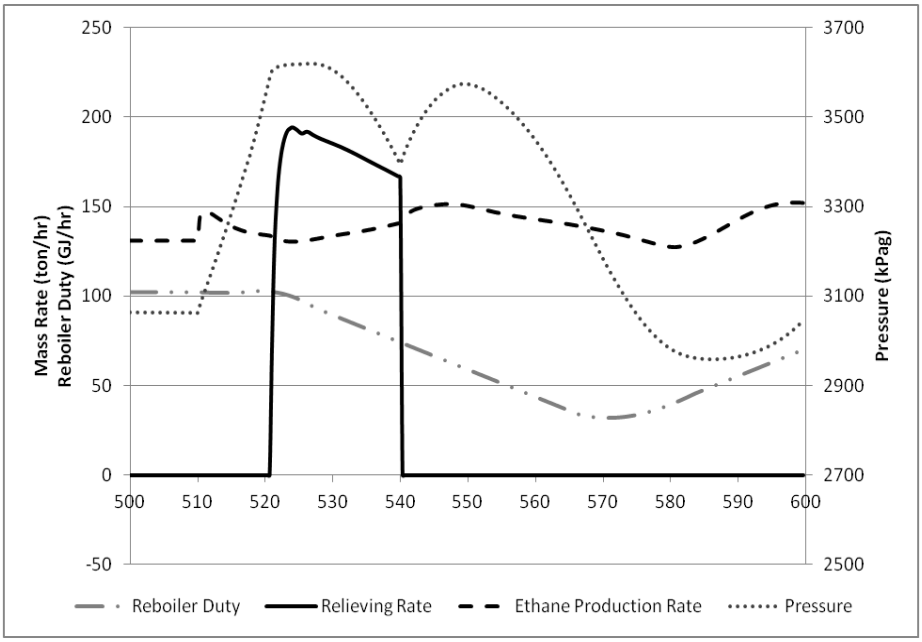

Figure 4.3 Dynamic simulation result of the condenser duty loss scenario for the ethane separation system

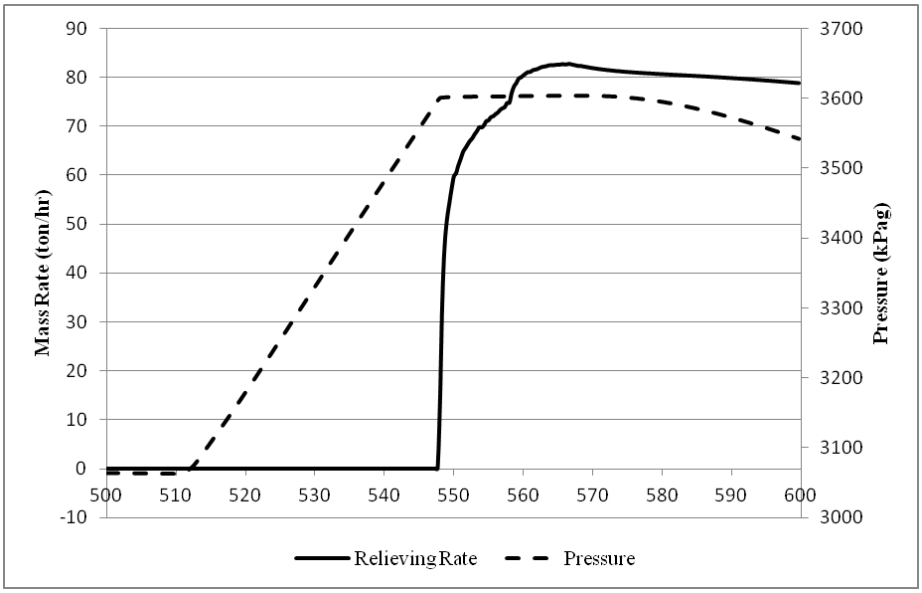

Figure 4.4 Dynamic simulation result of the abnormal heat input scenario for the ethane separation system

Table 4.5 Dynamic simulation results of the relief load estimation for the butane separation system and the isopentane separation system

Relief Scenario	The Butane Separation System	The Isopentane Separation System
Partial Power Failure (Blocked Outlets)	114.75 ton/hr	4.60 ton/hr
Condenser Duty Loss	66.02 ton/hr	4.19 ton/hr
Reflux Failure	0.00 ton/hr	0.00 ton/hr
Abnormal Heat Input	0.00 ton/hr	0.00 ton/hr

4.1.2. Relief Load Estimation from Multiple Sources

In this section, results of the relief load estimation from multiple sources by using a dynamic simulator will be presented. In order to simulate whole liquid fractionation unit, the steady-state model for the liquid fractionation unit was built. And then, the stabilization of the dynamic model for the liquid fractionation unit was performed. The result of the stabilization is shown in Figure 4.5. The mass flow rate and the purity of each product were stabilized at 900 minutes in simulation time.

Results of the relief load estimation from multiple sources when the general power failure happened are shown in Figures 4.6 to 4.7. As a result, there was no relief load from the isopentanizer and the relief did not occurred simultaneously in the deethanizer and the debutanizer.

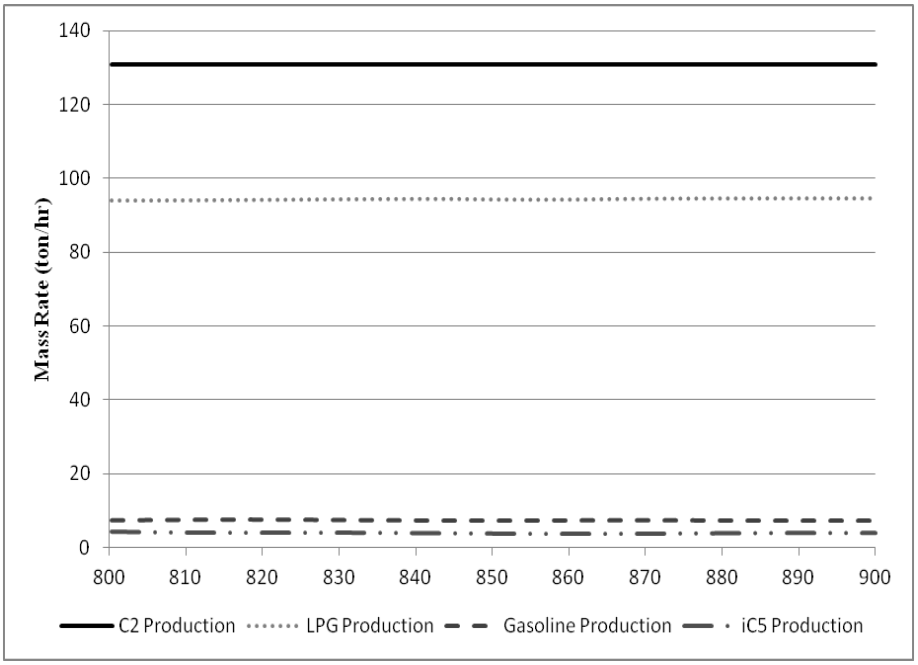

Figure 4.5 Stabilization result of the liquid fractionation unit

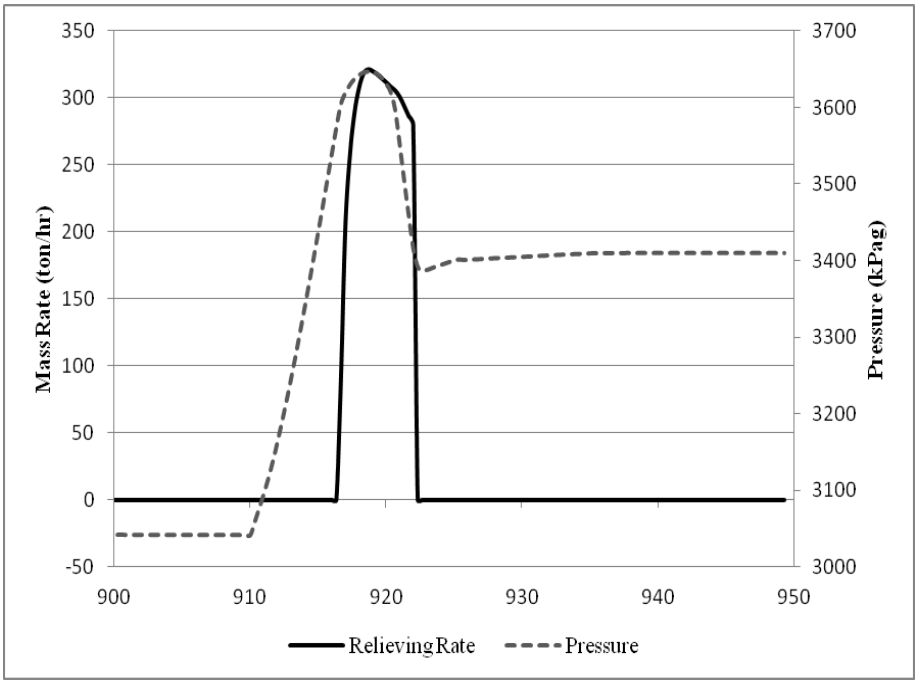

Figure 4.6 Dynamic simulation result for the ethane separation unit when the general power failure happened (320.92 ton/hr)

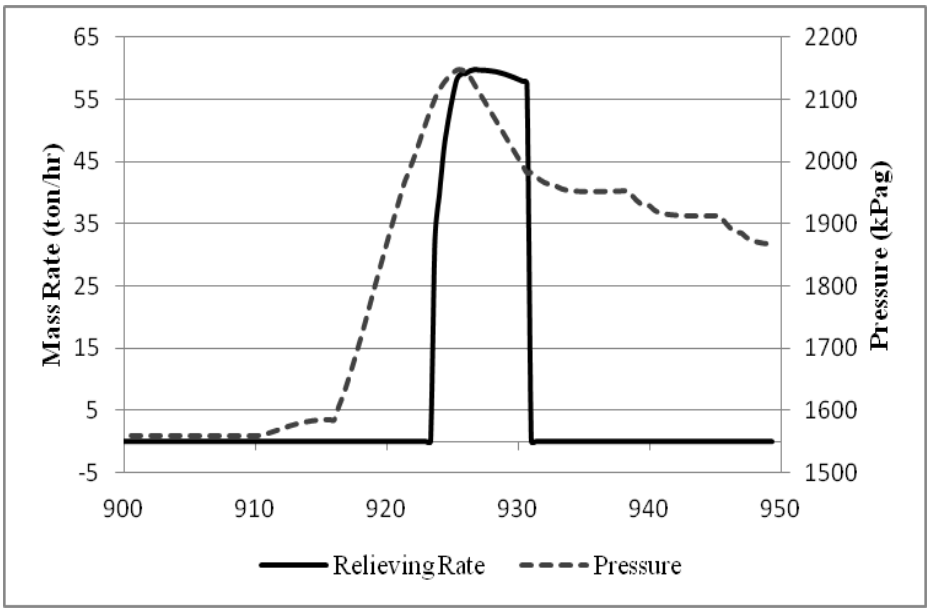

Figure 4.7 Dynamic simulation result for the butane separation unit when the general power failure happened (59.69 ton/hr)

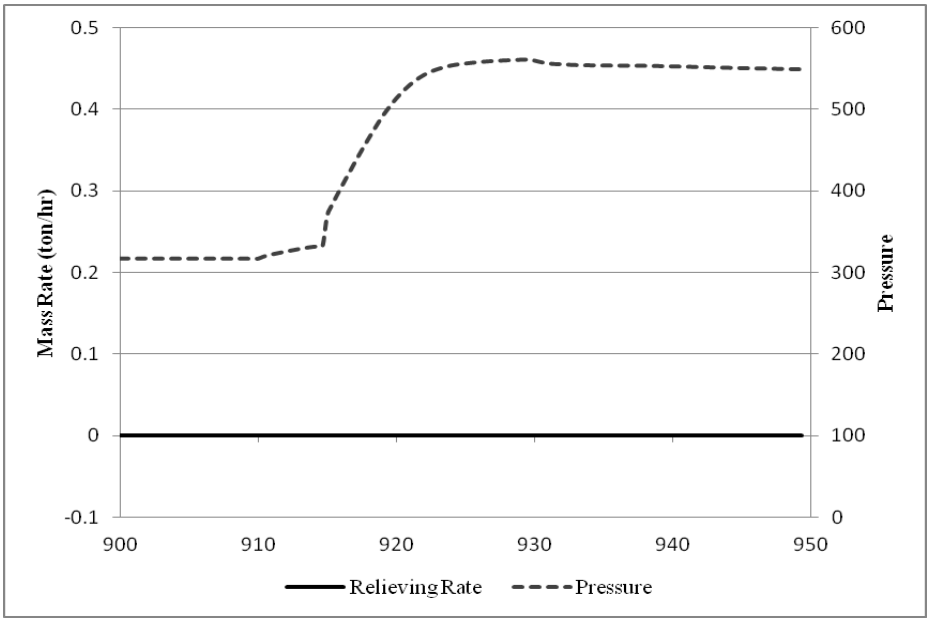

Figure 4.8 Dynamic simulation result for the isopentane separation unit when the general power failure happened (0 ton/hr)

4.1.3. Results Summary

Relief loads from a single source and multiple sources were simulated by using a dynamic simulator in this section. As a result, the general power failure scenario caused the maximum relief load for the liquid fractionation unit. The total amount of the maximum relief load was 320.92 ton/hr and this was the governing load for the whole liquid fractionation system and the ethane separation system.

The governing relief case for the butane separation unit and the isopentane separation unit were the Partial power failure scenario, and it caused 114.75 ton/hr and 4.60 ton/hr as a relief load, respectively. The relief load estimation results for the dynamic simulation are summarized in Table 4.6.

Table 4.6 Dynamic simulation results summary for the liquid fractionation unit

	Scenario	Relief Load
Liquid Fractionation Unit	General Power Failure	320.92 ton/hr
Ethane Separation Unit	General Power Failure	320.92 ton/hr
Butane Separation Unit	Partial Power Failure	114.75 ton/hr
Isopentane Separation Unit	Partial Power Failure	4.60 ton/hr

4.2. Relief Load Estimation for a Xylene Fractionation Unit and the PAREX unit

In this section, results of dynamic simulation runs in order to estimate the relief load for the xylene fractionation unit and the PAREX unit will be presented. The process flow diagram of the xylene fractionation unit and the PAREX unit is shown in Figure 3.4.

4.2.1. Relief Load Estimation from a Single Source

As stated earlier, the relief load estimation for the individual column was done by using the event scheduler in HYSYS. The dynamic simulation result for the individual column is summarized in Tables 4.7 to 4.10.

Table 4.7 Relief load estimation results by using a dynamic simulator for the 1st xylene splitter

Scenario	Relief Load
Partial Power Failure	416.06 ton/hr
Reflux Failure	350.75 ton/hr
Cooling Water Failure	448.13 ton/hr

Table 4.8 Relief load estimation results by using a dynamic simulator for the 2nd xylene splitter

Scenario	Relief Load
Overhead Pump Failure	945.26 ton/hr
Reflux Failure	893.84 ton/hr
1st Condenser Duty Lost	942.63 ton/hr
2nd Condenser Duty Lost	908.16 ton/hr

Table 4.9 Relief load estimation results by using a dynamic simulator for the 1st column in the PAREX unit

Scenario	Relief Load
Partial Power Failure	286.71 ton/hr
Reflux Failure	205.92 ton/hr
Cooling Water Failure	305.61 ton/hr
Condenser Duty Lost	135.93 ton/hr

Table 4.10 Relief load estimation results by using a dynamic simulator for the 2nd column in the PAREX unit

Scenario	Relief Load
Partial Power Failure	51.84 ton/hr
Reflux Failure	20.13 ton/hr
Air Fin Cooler Failure	0.00 ton/hr

4.2.2. Relief Load Estimation from Multiple Sources

In this section, results of the relief load estimation from multiple sources by using a dynamic simulator will be presented. In order to simulate the xylene fractionation and the PAREX unit, the steady-state model for simulate the xylene fractionation and the PAREX unit were built. And then, the stabilization of the dynamic model for the xylene fractionation and the PAREX unit was done. The result of the stabilization is shown in Figure 4.8.

The general power failure scenario and the cooling water failure scenario can cause the relief from multiple PSVs. In the case of the cooling water failure scenario, it does not need an additional simulation run since it is already performed in the stage of the relief load estimation from a single source. The total amount of relief load of the cooling water failure scenario is 753.74 ton/hr (448.13 ton/hr +305.61 ton/hr).

However, in the case of the general power failure scenario, an additional dynamic simulation run was performed. Results of the relief load estimation from multiple sources when the general power failure happened are shown in Figures 4.9 to 4.12. As a result, there are no relief occurred when the general power failure happened.

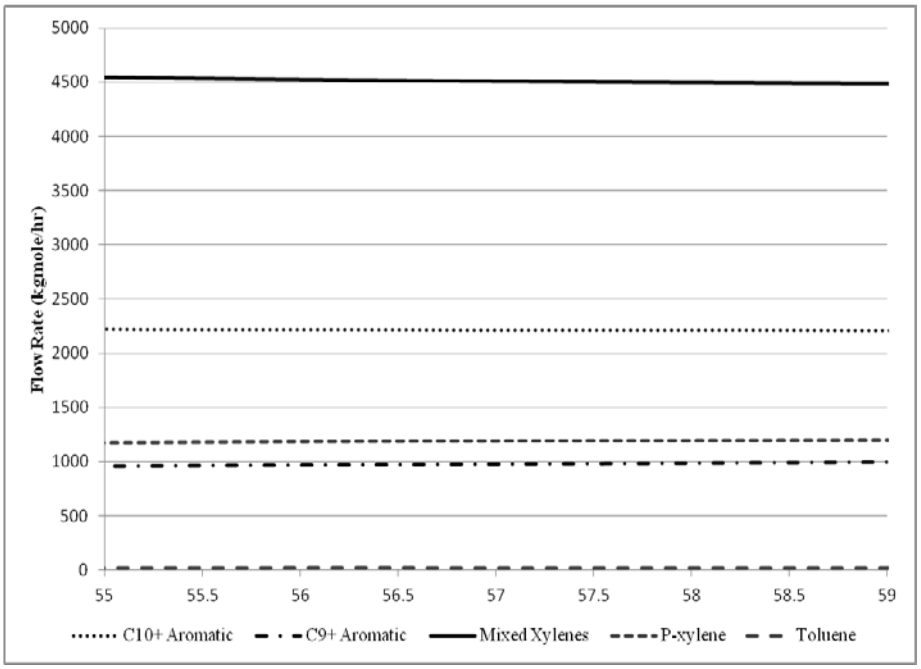

Figure 4.9 Stabilization results of the xylene fractionation and the PAREX unit

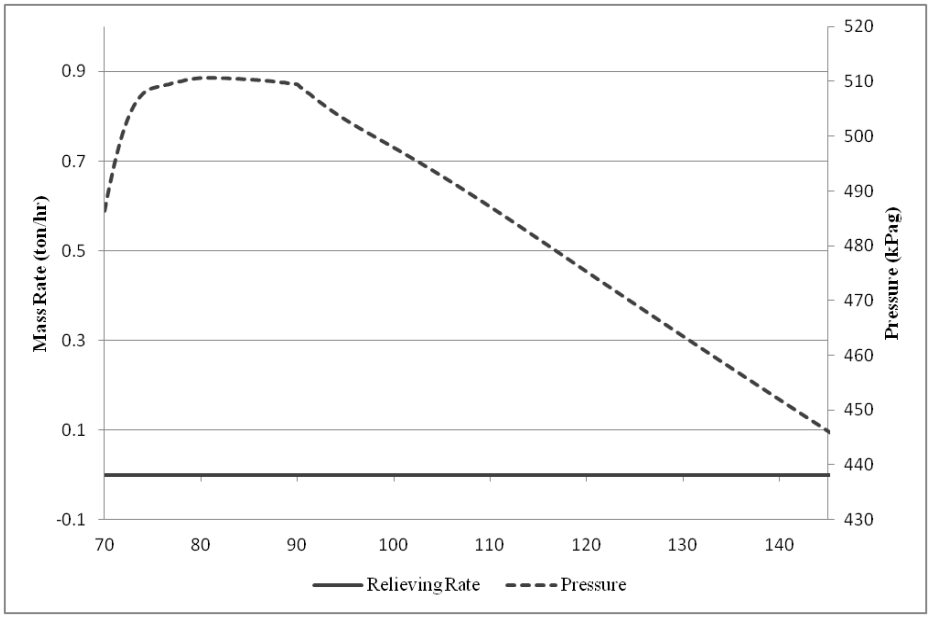

Figure 4.10 Dynamic simulation result for the 1st xylene splitter when the general power failure happened

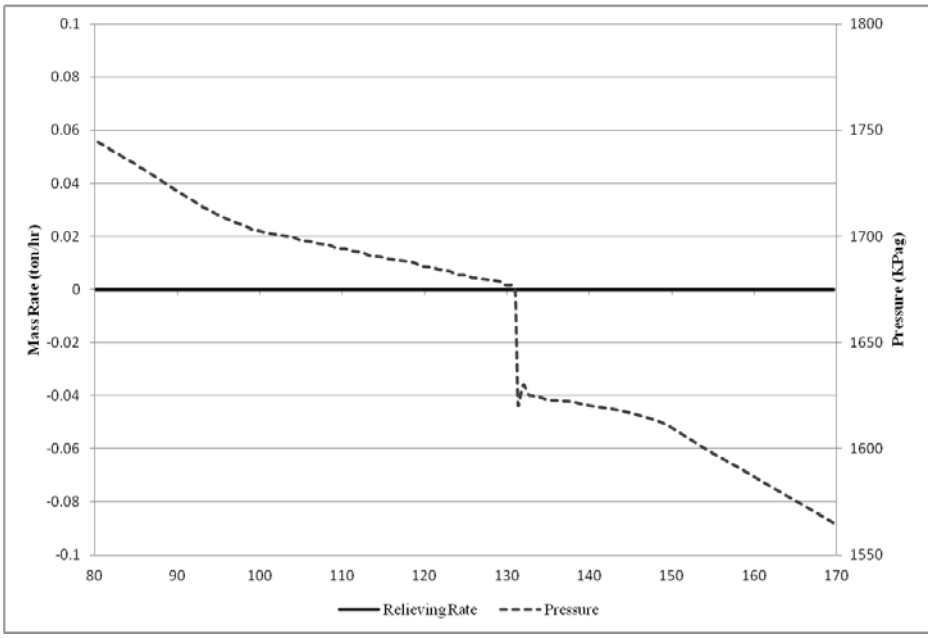

Figure 4.11 Dynamic simulation result for the 2nd xylene splitter when the general power failure happened

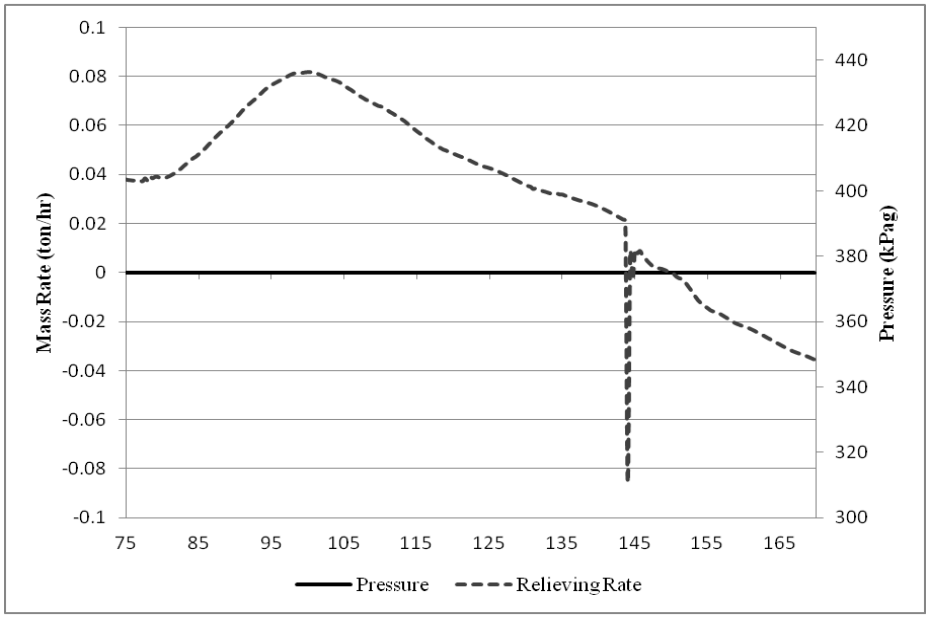

Figure 4.12 Dynamic simulation result for the 1st column in the PAREX unit when the general power failure happened

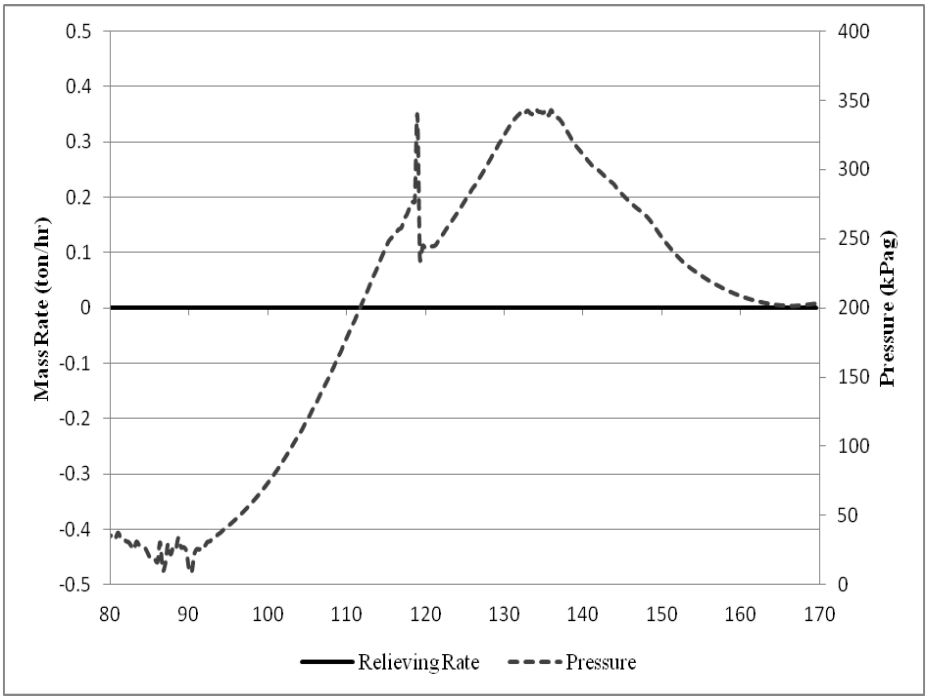

Figure 4.13 Dynamic simulation result for the 2nd column in the PAREX unit when the general power failure happened

4.2.3. Results Summary

Results of relief loads estimation from a single source and multiple sources for the xylene fractionation unit and the PAREX unit by using a dynamic simulator were presented in this section.

As a result, the 2nd xylene splitter caused the maximum relief load when the reflux failure occurred. The total amount of the maximum relief load was 945.26 ton/hr and this was the governing load for the xylene fractionation and the PAREX unit. The governing relief scenario for the each individual column is summarized in Table 4.11.

Table 4.11 Dynamic simulation results summary for the xylene fractionation and the PAREX unit

	Scenario	**Relief Load**
Governing Case	The overhead pump failure of the 2nd xylene column	945.26 ton/hr
1st xylene splitter	Cooling Water Failure	448.13 ton/hr
2nd xylene splitter	Overhead Pump Failure	945.26 ton/hr
1st column in the PAREX unit	Cooling Water Failure	305.61 ton/hr
2nd column in the PAREX unit	Partial Power Failure	51.84 ton/hr

5. Discussion Regarding Results of the Relief Load Estimation

5.1. The Liquid Fractionation Unit

Relief load estimations for the liquid fractionation unit were done using the heat and material balance method and the dynamic simulation. As a result, the maximum relief scenario for the liquid fractionation unit is the general power failure in both estimation methods. However, the estimation result of the maximum relief load shows a big difference between two estimation methods. For example, the maximum relief load is 1039.08 ton/hr in the heat and material balance method, whereas the maximum relief load is 320.92 ton/hr in the dynamic simulation. Governing relief cases and corresponding relief loads of both estimation methods are summarized in Table 4.12.

Table 5.1 Governing relief cases and corresponding relief loads of the liquid fractionation unit

	H&MB Method		Dynamic Simulator		Reduction Rate
	Scenario	Relief Load	Scenario	Relief Load	%
Whole Unit	General Power Failure	1039.08 ton/hr	General Power Failure	320.92 ton/hr	69.11
Ethane Separation System	General Power Failure	674.82 ton/hr	General Power Failure	320.92 ton/hr	52.44
Butane Separation System	General Power Failure	259.38 ton/hr	Partial Power Failure	114.75 ton/hr	55.76
i-C5 Separation System	General Power Failure	104.88 ton/hr	Partial Power Failure	4.60 ton/hr	95.61

5.2. The Xylene Fractionation Unit and the PAREX Unit

Relief load estimations for the xylene fractionation unit and the PAREX unit were done using the heat and material balance method and the dynamic simulation. As a result, the maximum relief scenario for the xylene fractionation unit and the PAREX unit is the overhead pump failure of the 2nd xylene splitter according to the result of dynamic simulation while the general power failure caused the maximum relief load according to the heat and material balance method. In addition, the maximum relief load is 945.26 ton/hr according to the result of the dynamic simulation while the maximum relief load is 1815.67 ton/hr according to the result of the heat and the material balance method. Governing relief cases and corresponding relief loads of both estimation methods are summarized in Table 4.13.

Table 5.2 Governing relief cases and corresponding relief loads of the xylene fractionation and the PAREX unit

	H&MB Method		Dynamic Simulator		Reduction Rate
	Scenario	**Relief Load**	**Scenario**	**Relief Load**	**%**
Whole Unit	The General Power Failure	1815.67 ton/hr	The overhead pump failure of the 2nd xylene column	945.26 ton/hr	47.94
1st xylene splitter	The General Power Failure	882.07 ton/hr	Cooling Water Failure	448.13 ton/hr	49.20
2nd xylene splitter	Overhead Pump Failure	1527.76 ton/hr	Overhead Pump Failure	945.26 ton/hr	38.13
1st column in the PAREX unit	The General Power Failure	694.38 ton/hr	Cooling Water Failure	305.61 ton/hr	55.99
2nd column in the PAREX unit	The General Power Failure	239.22 ton/hr	Partial Power Failure	51.84 ton/hr	78.33

5.3. Discussion

As presented earlier, the maximum relief load which was estimated by using the dynamic simulator is less than that of the heat and material balance method. This result is caused by the several big differences between two estimation methods. First, the heat and material balance method does not account for control actions at all while the dynamic simulation does account for control actions. For example, we can find that the heat input was controlled when the reflux failure occurred in the dynamic simulation results. However, we assumed the heat input would be maintained same as the normal duty in the heat and material balance method.

Second, the dynamic simulation can estimate the changes in the material balance. For instance, we can find changes in the mass rate of ethane production in Figure 4.3. However, we assumed the ethane production rate would not be changed after the condenser duty loss occurred in the heat and material balance method.

Third, the dynamic simulation can simulate the timeline of all scenarios. It is very helpful to estimate the relief load precisely. For example, the total relief load for the general power failure is 380.61 ton/hr in the dynamic simulation, but the maximum relief load is 320.92 ton/hr since reliefs from C2 tower and C3 tower does not occur

simultaneously. Unfortunately, the heat and material balance method cannot provide those insights.

Finally, the dynamic simulation can simulate interactions between equipments. For instance, we assumed the feed flow rate would be zero for the butane separation unit in the heat and material balance method. However, the feed for the butane will be continued until the level of deethanizer sump goes down to the low-low level. If the feed is continued and sub-cooled, the relief load can be reduced since the heat from the reboiler will be used to heat the feed up. In addition, the general power failure caused no relief at all in the dynamic simulation of the xylene fractionation unit and the PAREX unit although the governing relief scenario was the general power failure in the heat and the material balance method. The reason why the dynamic simulation is can calculate the exact heat duty of heat exchanger which use process vapor as the heating medium.

In conclusion, the relief load estimation method using the heat and material balance is too conservative and tends to overestimate the relief load since it is a steady state method while overpressure events are dynamic events. On the other hands, the relief load can be estimated more reasonably using the dynamic simulation than using the heat and material balance method since the dynamic simulation is suitable method to illustrate the overpressure event.

6. Relief Load Mitigation Using HIPS

6.1. General Description

In conventional design, a pressure relief valve (PRV) is used as the primary means of protection according to API and ASME code. However, the use of a PRV is sometimes an unattractive, particularly when the flare load is large. API STD 521 allows the use of a safety instrument system (SIS) instead of a PRV as long as the SIS meets or exceeds the protection that would have been provided by a PRV. SIS which meets or exceeds the safety availability of a PRV is often called high integrity protection systems (HIPS).

HIPS can be used to provide overpressure protection if a quantitative or qualitative risk analysis of the proposed system is made addressing credible overpressure scenarios. It must be demonstrated that the proposed HIPS is as reliable as the PRV it replaces and is capable of completely mitigating the overpressure event. And the process dynamics must be evaluated to ensure that the HIPS response time is fast enough to prevent overpressure of the equipment.

6.2. HIPS Application to the Liquid Fractionation Unit

As stated earlier, HIPS can reduce the probability that several relief devices will have to operate simultaneously, thereby allowing for a reduction in the size of the disposal system. In this research, the general power failure scenario involved multiple PRVs and caused the maximum relief load in both estimations, which are the heat and material balance method and the estimation by using a dynamic simulator.

Therefore, HIPS can eliminate the general power failure case if HIPS satisfy the availability which can be provided by PRVs. As indicated in Table 2.2, the availability of HIPS should satisfy the SIL3 in order to eliminate the general power failure scenario since the PFD of the PRV lies between SIL2 and SIL 3. If we use the heat and material balance method in order to implement HIPS, HIPS should be applied each system since the relief will occur in each column. The scheme of HIPS implementation by the heat and material balance method for the liquid fractionation system is shown in Figures 6.1 and 6.2.

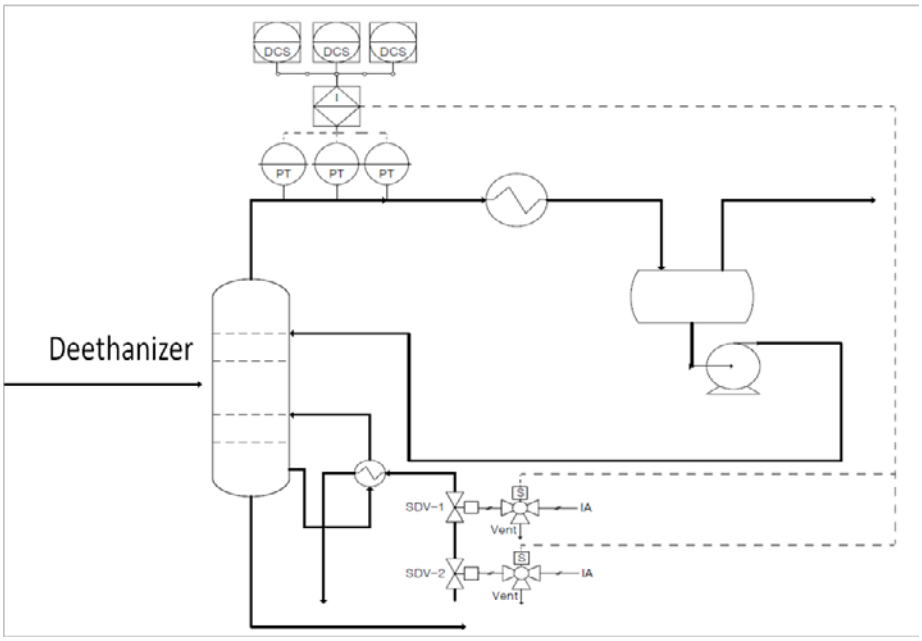

Figure 6.1 HIPS configuration for the ethane separation system

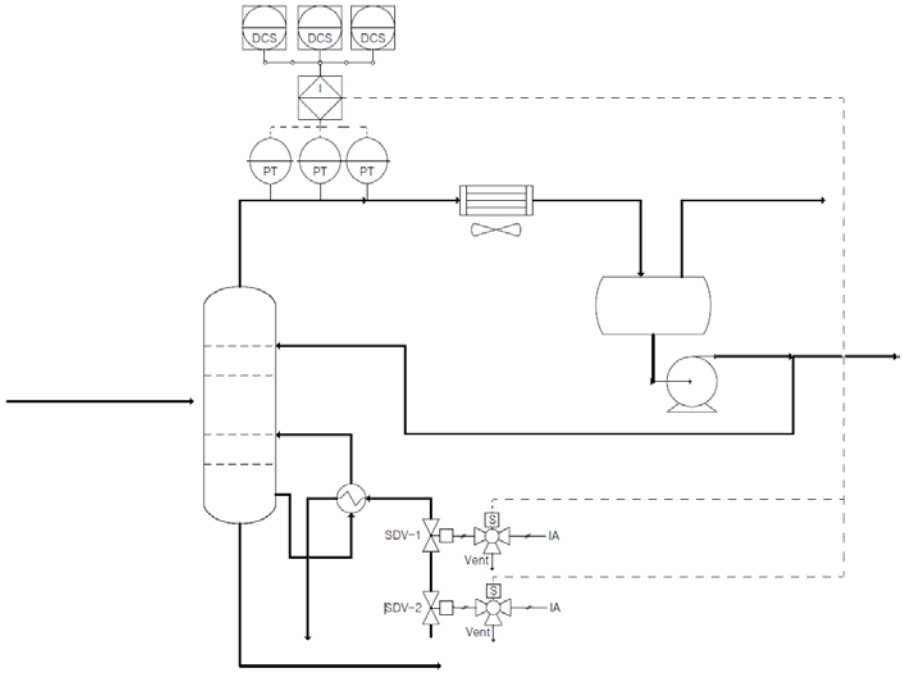

Figure 6.2 HIPS configuration for the butane and isopentane separation system

However, if we use a dynamic simulator in order to implement HIPS, the HIPS configuration can be optimized. The results of dynamic simulation when HIPS was implemented only in the ethane separation system are shown in Figures 6.3 to 6.5. If HIPS was applied to the ethane system only, the relief occurred in the butane and isopentane separation system and relief loads are 37.26 ton/hr and 19.34 ton/hr, respectively. The load from the butane separation system can be covered by the existing PRV. But the load from the isopentane separation system cannot be covered by the existing PRV. This problem can be solved by enlarging the orifice size of PRV from H to L and the size of in/out pipe [47]. That is more cost effective than the implementation of additional HIPS since HIPS include two emergency shutdown valves.

Furthermore, the process engineer can figure out the optimal alarm set point and the required response time of HIPS through the result of dynamic simulation. Consequently, the process engineer can design the plant more robustly as preventing the unnecessary plant shut down and ensuring HIPS performance.

Time (min.)	Action
910	The event happened
913.5	PAHH (3300 kPag)
913.5~915	Signal Processing
915	Control valve started to close.
916	Control valve closed.

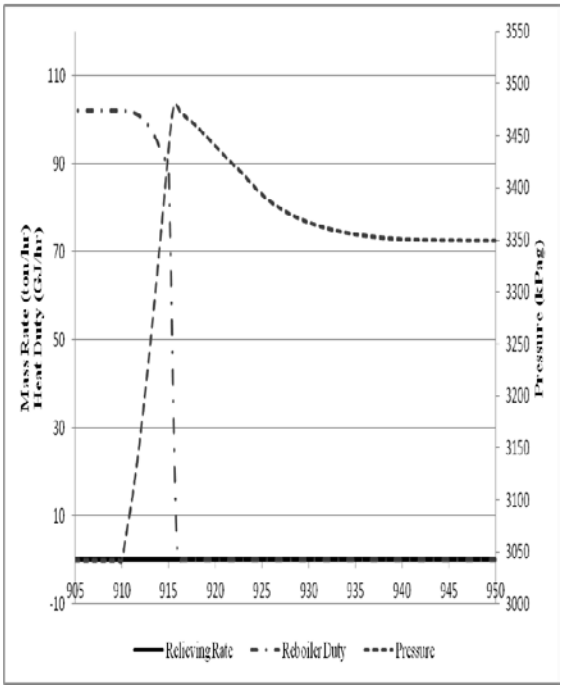

Figure 6.3 Dynamic simulation result for the ethane separation unit when HIPS implemented in the ethane separation system only

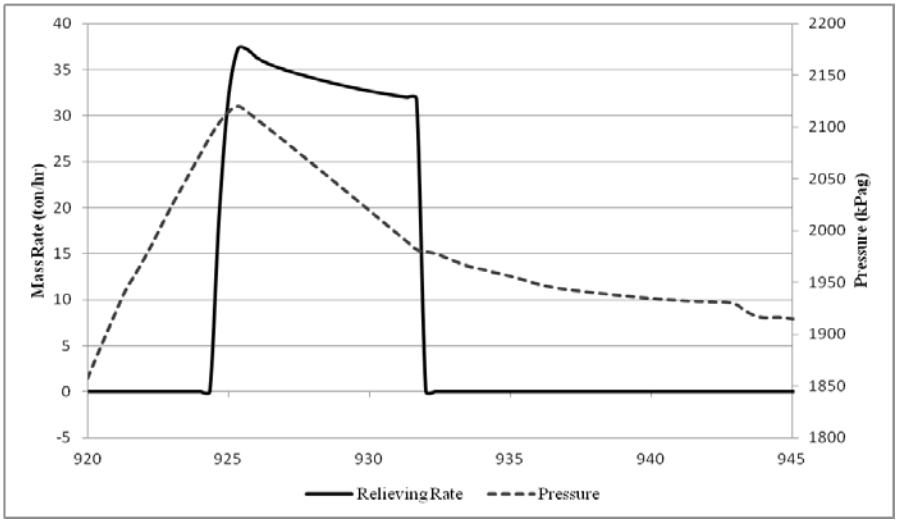

Figure 6.4 Dynamic simulation result for the butane separation unit when HIPS implemented in the ethane separation system only

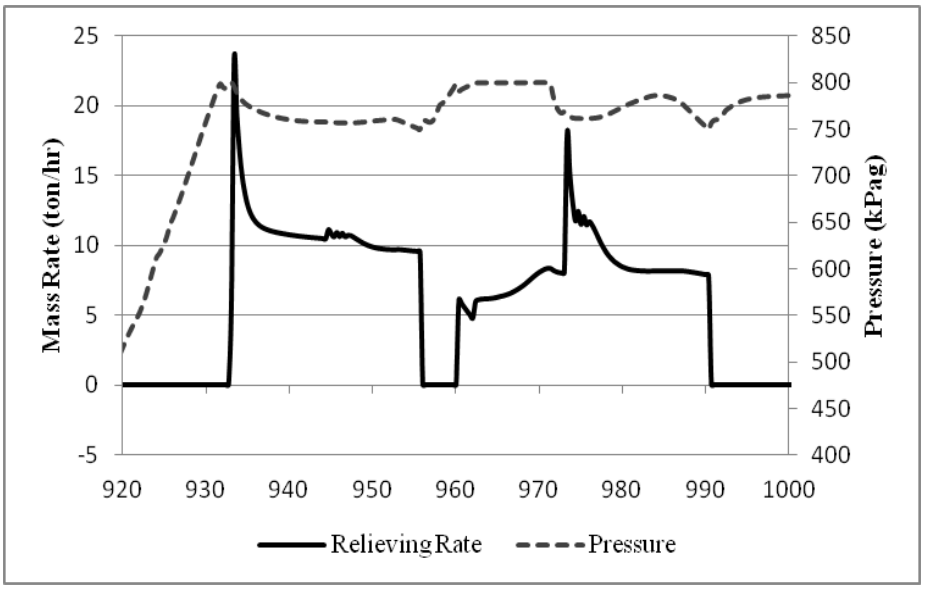

Figure 6.5 Dynamic simulation result for the isopentane separation unit when HIPS implemented in the ethane separation system only

And fault tree analysis (FTA) was done in order to ensure the PFD of the proposed system satisfy SIL3. As a result, the PFD of proposed system is $3.79*10^{-4}$ and this satisfies SIL3. The dangerous failure rate of each sub system was from OREDA handbook [29]. The result of FTA is shown in Figure 6.6.

By implementing HIPS, the governing relief load is reduced from 320.92 ton/hr to 234.85 ton/hr since the governing relief scenario is changed from the general power failure scenario to the reflux failure of the ethane separation system scenario.

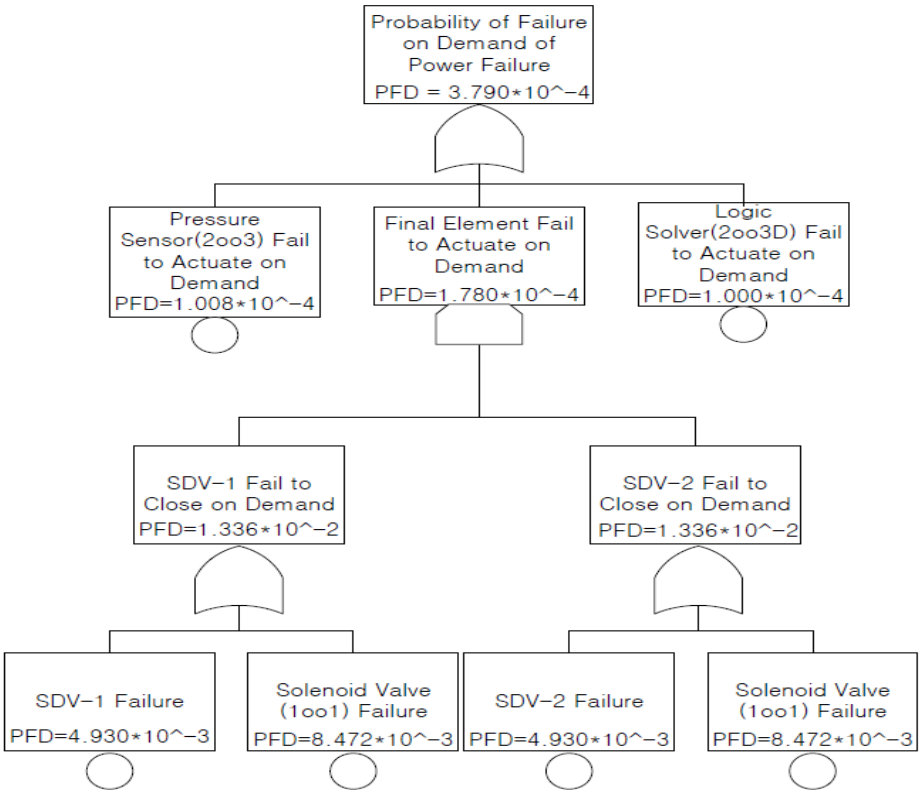

Figure 6.6 Result of FTA analysis

7. The Effect of the Dynamic Simulation implementation for the Flare System Design

7.1. Proper Design Stage for the Estimation of the Relief Load

In this section, the effect of the dynamic simulation in the flare system design will be investigated. In order to estimate the relief load of a certain process, some process information is needed such. In the case of the heat and the material balance method, the heat and the material balance of in/out streams, heat duties of heat exchangers and thermodynamic data of in/out streams are needed for calculating the relief load.

However, in the case of a dynamic simulation, more information is needed than that of the heat and the material balance method since it is a more complex and time consuming work than the estimation method by using the heat and the material balance method. For instance, in order to perform a dynamic simulation, size data of equipment, performance curves of pumps or compressors, size data of valves, control parameters of controllers and etc.

Therefore, the relief load estimation cannot be conducted in the early stage of a plant design. Design steps of a plant design are shown in Figure 7.1. As shown in Figure 7.1, required information for estimating the relief load can be prepared after front end engineering design (FEED) stage regardless of estimation method. In principle, the heat and material balance and equipment design data are not changed in the detailed design stage, the relief load estimation after FEED stage can have a sufficient reliability. Consequently, the execution of the dynamic simulation for the estimation of the relief load also has a sufficient reliability for its results.

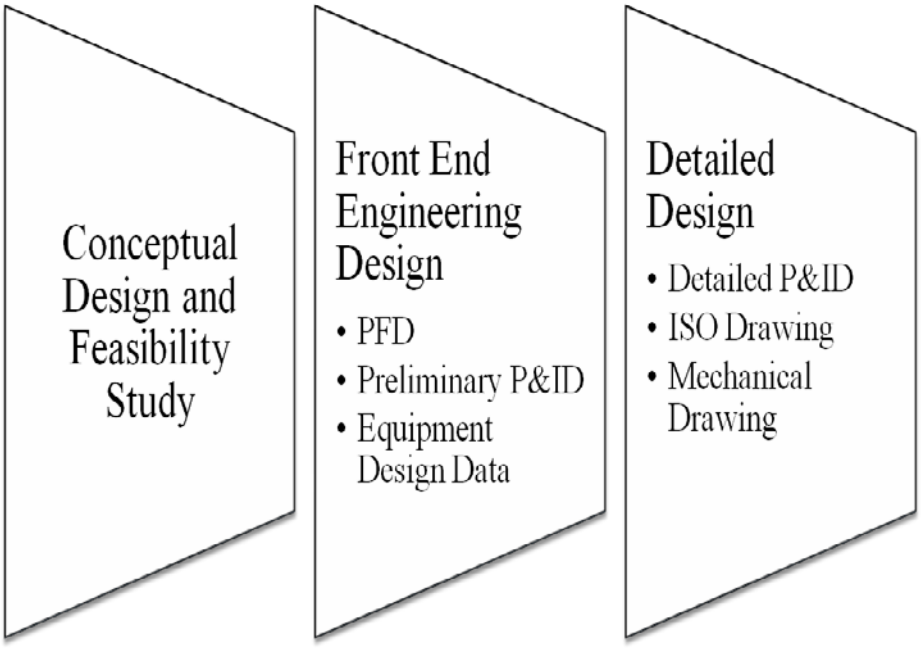

Figure 7.1 Design steps of a plant design

7.2. Cost Effect of the Dynamic Simulation

In this section, the cost effect of the relief load reduction by using a dynamic simulator for the flare design will be analyzed.

As investigated earlier, the governing relief loads by estimating through the dynamic simulation tend to have smaller value than those of the heat and the material balance method. Reduction rates of the relief load according to the dynamic simulation result are summarized in Table 7.1.

These results are very crucial to the flare system design since the flare header which is the most cost effective part of the flare system design, directly affected by the governing relief load. In order to quantify the cost effect of dynamic simulation, preliminary sizing of the flare header was performed [35]. Results of preliminary flare header design and its estimated material cost are summarized in Table 7.2.

Table 7.1 Reduction rates of the relief load in the dynamic simulation

Unit	H&MB Method	Dynamic Simulation	Reduction Rate (%)
The Liquid Fractionation Unit	1039.08 ton/hr	320.92 ton/hr	69.11 %
The Xylene Fractionation and the PAREX Unit	1815.67 ton/hr	945.26 ton/hr	47.94 %

Table 7.2 Results of preliminary flare header design and its estimated material cost

	H&MB Method		Dynamic Simulator		Cost Reduction Rate
Unit	Header Size (inch)	Estimated Cost (MM US $)	Header Size (inch)	Estimated Cost (MM US $)	%
The Liquid Fractionation Unit	46	3.19	28	1.18	63.00
The Xylene Fractionation and the PAREX Unit	46	3.19	36	1.95	38.87

a. The construction material is carbon steel.

b. The density of carbon steel (CS) is assumed as 7850 kg/m^3.

c. The price of CS pipe is assumed as 794$/ton.

d. The equivalent length of the flare header is assumed as 1,500m.

e. Mach No. at the flare header is limited to 0.5.

As shown in Table 7.2, estimated material costs of flare headers is reduced over 1 million dollars in both cases by using results of dynamic simulations. Therefore, the execution of the dynamic simulation for calculating the relief load brings a great economical advantages since the cost of dynamic simulation is around 0.1 million dollars.

In the case of HIPS implementation, the exact cost comparison was not performed due to the lack of cost information of HIPS. However, by implementing HIPS, the size of flare header for the liquid fractionation unit is reduced to 24 inch and its estimated material cost is reduced to 0.87 MM US $ in the case of the liquid fractionation unit. In addition, by combining HIPS and the dynamic simulation, the configuration of HIPS became much simple. Results of simplified HIPS configuration by combining HIPS and the dynamic simulation are summarized in Table 7.3. Therefore, if the cost of simplified HIPS is less than 0.31 MM US $, implementation of HIPS should be considered.

Table 7.3 Results of simplified HIPS configuration by combining HIPS and the dynamic simulation

	Original HIPS	Simplified HIPS
No. of ESD valves	6	2
No. of Solenoid valves	6	3
No. of Pressure transmitters	9	3
No. of Logic solvers	9	3

As discussed above, the implementation of the dynamic simulation for the flare system design can bring economical advantages. However, the implementation of the dynamic simulation for all relief scenarios is impractical since it is an extremely time-consuming work. Therefore, the dynamic simulation should be conducted in order to reduce the relief load of the governing relief scenario. The characteristics of each relief load estimation method are summarized in Table 7.4. And the new design procedure for the efficient flare system design is shown in Figure 7.2.

Table 7.4 Characteristics of Relief Load Estimation Methods

H&MB method	Dynamic Simulation
1. Less time-consuming. 2. Proper method to handle whole flare system. 3. Advantages for the preliminary flare system design. 4. Conservative.	1. Time-consuming. 2. Proper method to optimize flare system by reducing the maximum relief load. 3. Advantages for the rigorous flare system design. 4. Rigorous.

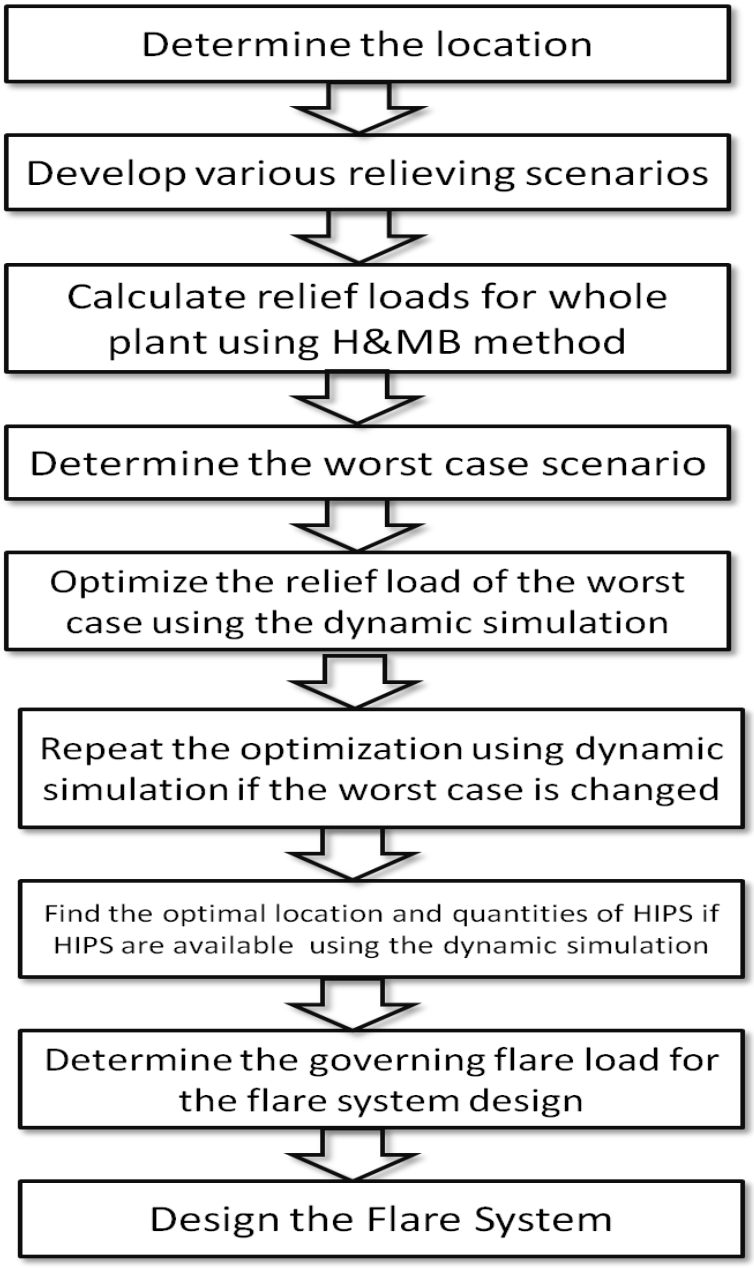

Figure 7.2 New Design Procedure for the Efficient Flare System Design

8. Conclusion

In this paper, the relief load estimation has been performed in order to design the flare system. The existing method which is based on API standard and the heat and material balance, and the new method based on the implementation of the dynamic simulation have been introduced as the relief load estimation method. And the liquid fractionation unit, and the xylene fractionation and the PAREX unit were studied.

As a result, relief loads which were estimated by using a dynamic simulator tends to have smaller values than those of the heat and material balance method. The design flare load was reduced by 69.11% in the case of a liquid fractionation unit and 47.94% in the case of a xylene fractionation and a PAREX unit. Consequently, the material cost of the flare header reduced more than 1 million dollars in both illustrated cases. In addition, the HIPS were introduced as the relief load mitigation method. And this research proved that dynamic simulation can evaluate performance of HIPS. Furthermore, the configuration of HIPS was simplified by combining the dynamic simulation and HIPS in the liquid fractionation unit.

However, the implementation of the dynamic simulation for all possible relief scenarios is impractical since it is highly time-

consuming work. Therefore, the implementation of the dynamic simulation should be carefully decided in the flare system design. Generally, the engineering work for the plant design is highly pressed for time. Consequently, the implementation of the dynamic simulation for the flare system design may not be attractive if process engineers try to simulate all relief scenarios or whole plant.

Nevertheless, process engineers can find the optimal way for the flare system design by following new design procedure which is suggested in this research. In the preliminary design stage of the flare system, the heat and material balance method will be suitable since it is conservative and less time-consuming. After the preliminary flare system design is finished, the governing relief load needs to be re-estimated by using a dynamic simulator in order to optimize the flare system design. By doing so, process engineers can optimize the flare system design in time.

The results obtained in this study can be of value to process engineers who design the flare system. The contributions of this research are as follows.

1. This research successfully proved that the relief load can be estimated more rigorously by using a dynamic simulator for column system.

2. The design flare load was reduced by 69.11% in the case of a liquid fractionation unit and 47.94% in the case of a xylene fractionation and a PAREX unit through dynamic simulation.
3. The estimated material construction cost was reduced by 63% in the case of a liquid fractionation unit and 38.87% in the case of a xylene fractionation and a PAREX unit through dynamic simulation.
4. The design flare load was reduced by 26.82% when HIPS was implemented.
5. This research successfully proved that the configuration of HIPS can be simplified using dynamic simulation.
6. This research suggested the new design procedure for the efficient flare system design as combining existing code based method and dynamic simulation.

References

[1] J. M. Douglas, Conceptual Design of Chemical Processes, McGraw-Hill, 1988.

[2] API, API Standard 521 “Guide for Pressure Relieving and Depressuring Systems”, 5th edition, 2008.

[3] API, API Standard 520 “ Sizing, Selection, and Installation of Pressure-relieving Devices in Refineries Part I – Sizing and Selection”, 8th edition, 2008.

[4] API, API Recommended Practice 520 “ Sizing, Selection, and Installation of Pressure-relieving Devices in Refineries Part II – Installation”, 5th edition, 2003.

[5] J. R. Cassata, S. Dasgupta and S. L. Gandhi, Modeling of tower relief dynamics, Hydrocarbon Processing, October, 71-76, 1993.

[6] V. Patel, J. Feng, S. Dasgupta and J. Kramer, Use of Dynamic Simulation in the Design of Ethylene Plants, the 20th Ethylene Producers’ Conference 2008, 2008.

[7] A. E. Summers, Flare Load Mitigation Using High Integrity Protection Systems (HIPS), ISA Expo 2003, 2003.

[8] D. A. Crwol and J. F. Louvar, Chemical Process Safety : Fundamentals with Applications, 2nd edition, Prentice Hall, 2004.

[9] W. L. Luyben, Plantwide Dynimic Simulators in Chemical Processing and Control, Marcel Dekker, Inc., 2002.

[10] Aspen Technology, Inc. Aspen HYSYS – Dynamic Modeling Guide, Aspen Technology, Inc., 2011.

[11] BSI, BS EN 61508-1:2010 “Functional safety of electrical/electronic/programmable electronic safety-related systems Part 1 : General requirements”, 2010.

[12] BSI, BS EN 61508-2:2010 “Functional safety of electrical/electronic/programmable electronic safety-related systems Part 2 : Requirements for electrical/electronic/ programmable electronic safety-related systems”, 2010.

[13] BSI, BS EN 61508-3:2010 “Functional safety of electrical/electronic/programmable electronic safety-related systems Part 3 : Software requirements”, 2010.

[14] BSI, BS EN 61508-4:2010 “Functional safety of electrical/electronic/programmable electronic safety-related systems Part 4 : Definitions and abbreviations”, 2010.

[15] BSI, BS EN 61508-5:2010 “Functional safety of electrical/electronic/programmable electronic safety-related systems Part 5 : Examples of methods for the determination of safety integrity levels”, 2010.

[16] BSI, BS EN 61508-6:2010 “Functional safety of electrical/electronic/programmable electronic safety-related systems Part 6 : Guidelines on the application of IEC 61508-2 and

IEC 61508-3”, 2010.

[17] BSI, BS EN 61508-7:2010 “Functional safety of electrical/electronic/programmable electronic safety-related systems Part 7 : Overview of techniques and measures”, 2010.

[18] BSI, BS EN 61511-1:2004 “Functional safety – Safety instrumented systems for the process industry sector – Part 1 : Framework, definitions, system, hardware and software requirements”, 2004.

[19] BSI, BS EN 61511-2:2004 “Functional safety – Safety instrumented systems for the process industry sector – Part 2 : Guidelines for the application of IEC 61511-1”, 2004.

[20] CCPS, Guidelines for Process Equipment Reliability Data - with Data Tables, John Wiley & Sons Inc., 1989.

[21] J. S. Ko and H. Kim, Reliability Analysis on Safety Instrumented System of High Density Polyethylene Plant, Theories and Applications of Chem. Eng., vol.11, No. 2, 2005.

[22] CCPS, Guidelines for Chemical Process Quantitative Risk Analysis, 2nd edition, 2000.

[23] D. F. Hassl, Advanced Concepts in Fault Tree Analysis, System Safety Symposium, 1965.

[24] N. C. Rasmussen, Reactor Safety Study: An Assessment of Accident Risk in U.S. Nuclear Power Plants, Nuclear Regulatory

Commission, 1975.

[25] CCPS, Guidelines for Investigating Chemical Process Incidents, 2nd edition, 2003.

[26] A. C. Dimian, Integrated Design and Simulation of Chemical Processes, Elsevier, 2003.

[27] W. L. Luyben, Process Modeling, Simulation, and Control for Chemical Engineers, McGraw-Hill, 1990.

[28] W. L. Luyben, Distillation Design and Control Using Aspen Simulation, John Wiley & Sons, Inc., 2006.

[29] SINTEF, Offshore Reliability Data, 3rd edition, Norway, 2002.

[30] A. Bagdasaryan, Discrete dynamic simulation models and technique for complex control systems, Simulation Modeling Practice and Theory, 19, 1061-1087, 2011.

[31] R. K. Goyal and E. G. Al-Ansari, Impact of emergency shutdown devices on relief system sizing and design, Journal of Loss Prevention in the Process Industries, 22, 35-44, 2009.

[32] P. M. Stoop, J. P. A. van den Bogaard and H. Koning, Int. J. Ves. & Piping, 18, 183-208, 1985.

[33] C.M. Jan, Dynamic Effects on Structures and Equipment Due to Safety Relief Valve Discharge Loads, Nuclear Engineering and Design 59, 171-183, 1980.

[34] J. R. Couper, W. R. Penney, J. R. Fair and S. M. Walas, Chemical

Process Equipment: Selection and Design, 2nd edition, Butterworth-Heinemann, 2010.

[35] C. R. Branan, Rules of Thumb for Chemical Engineers, 4th edition, Gulf Professional Publishing, 2005.

[36] W. D. Seider, J. D. Seader, D. R. Lewin and S. Widagdo, 3rd edition, John Wiley & Sons, Inc. 2009.

[37] P. D. T. O'Connor, Practical Reliability Engineering, 4th edition, John Wiley & Sons, Inc. 2002.

[38] P. Gruhn and H. Cheddie, Safety Instrumented Systems : Design, Analysis and Justification, 2nd edition, The Instrumentation, Systems, and Automation Society, 2006.

[39] R. Haberman, Applied Partial Differential Equations with Fourier Series and Boundary Value Problems, 4th education, Pearson Eduaction, Inc., 2004.

[40] G. H. Kim, Automatic Synthesis of Robust Accident Scenarios for Chemical Processes, Seoul National University, 2000.

[41] Y. H. Kim, A Study on Integrated Decision-Making System for Sequential Risk Assessment in Chemical Processes, Seoul National University, 2006.

[42] T. S. Kang, The Process Fault Diagnostic System Based on Multi-Agents and Function-Behavior Modeling, Seoul National University, 2000.

[43] J. C. Seo, Multi-Model Approach to Automated Hazard Analysis of Chemical Plants, Seoul National University, 1997.

[44] K. S. Kim, Development of the Real-time Risk Monitoring System for Chemical Plants, Kwangwoon University, 1999.

[45] A Study on Fault Diagnosis in Continuous Chemical Processes Using the Extended Symptom-Fault Association Model, Seoul National University, 1995.

[46] K. Dasgupta and J. Watton, Dynamic analysis of proportional solenoid controlled piloted relief valve by bondgraph, Simulation Modeling Practice and Theory, 13, 21-38, 2005.

[47] J. Cremers, K. Friedel and B. Pallaks, Validated sizing rule against chatter of relief valves during gas service, Journal of Loss Prevention in the Process Industries, 14, 261-267, 2001.

[48] T. Bjørge and A. Bratseth, Measurement of radiation heat flux from large scale flares, Journal of Hazardous Materials, 46, 159-168, 1996.

[49] B. W. Bequette, Process Control: Modeling, Design, and Simulation, Pearson Education, Inc., 2003.

[50] B. W. Bequette, Process Dynamics: Modeling, Analysis, and Simulation, Prentice Hall, 1998.

요약(국문초록)

산업계에서 합리적인 배출 용량의 예측은 전체 플레어 시스템 디자인에 영향을 미치는 아주 중요한 작업이다. 일반적으로 플레어 시스템은 아주 거대하고, 설치 비용이 많이 드는 시스템이기 때문에 만약, 방출 용량이 과잉 예측된다면 자원의 낭비를 피할 수가 없다. 하지만, 플레어 시스템은 공장의 안전 운전을 위한 최후의 물리적 보호 수단이므로, 방출 용량의 과소 예측으로 인해 적절하지 않은 크기로 설계된다면 끔찍한 사고를 불러일으킬 수도 있다.

따라서, 적절한 방출 용량 예측을 위해 미국석유협회에서는 API STD 520 및 521 을 통해 방출 용량 예측에 관한 설계 지침을 세우기 위해 노력해왔다. 하지만, 이 지침은 관점에 따라 다양하게 해석될 수 있다. 산업계에서는 열 및 물질 전달 수지식을 이용하여 논리적으로 방출 용량을 예측하는 방법이 보편적으로 사용되고 있다. 그러나, 이 방법은 매우 보수적인 예측 방법으로 방출 용량을 과잉 예측하는 경향이 있다.

최근에는 동적 모사 소프트웨어 및 컴퓨터 하드웨어의 발전으로 인해, 동적 모사를 이용하여 방출 용량을 예측하려는 시도가 이루어지고 있다. 동적 모사기를 이용한 화학공정의 모사는 정상 상태뿐 아니라, 비정상 상태에 대한

모사도 가능하다. 화학 공정에서 방출은 불안정한 상태하에서 이루어지므로, 동적 모사기를 이용한 방출 용량은 예측은, 기존 방법들에 비해 좀 더 정확하고 정교한 예측 결과를 산출해 낼 것이라고 기대된다.

이번 연구에서는 열 및 물질 전달 수지식 및 동적 모사기를 이용한 방출 용량 예측을 수행하였다. 또한, 방출 용량 감소를 위한 고도 융합 보호 체계 (HIPS) 와 동적 모사의 결합에 관한 연구도 진행하였다. 사례 연구를 위해, 액체 분리 공정 및 자일렌 분리 공정 (PAREX 공정 포함) 이 선택되었다. 마지막으로, 효율적인 플레어 시스템 설계를 위한 새로운 방법론도 제안하였다.

주요어: 플레어 설계, 방출 용량 예측, 동적 모사, 고도 융합 보호 체계 (HIPS)

학번: 2008-21074 **성 명: 박경태**